Molecular Regulation of Direct Cardiac Reprogramming

APPROVED BY SUPERVISORY COMMITTEE

Committee Chairperson _____
Chun-Li Zhang, PhD

Committee Member _____
Joseph Hill, MD/PhD

Committee Member _____
Ondine Cleaver, PhD

Committee Member _____
Eric N. Olson, PhD

DEDICATION

To my family for all their support

&

To my wife
for always being there for me

Molecular Regulation of Direct Cardiac Reprogramming

by

Huanyu Zhou

DISSERTATION

Presented to the Faculty of the Graduate School of Biomedical Sciences

The University of Texas Southwestern Medical Center at Dallas

In Partial Fulfillment of the Requirements

For the Degree of

DOCTOR OF PHILOSOPHY

The University of Texas Southwestern Medical Center at Dallas

Dallas, Texas

August, 2017

ACKNOWLEDGEMENTS

There are so many people I would like to thank for making my years in Dallas so fruitful and enjoyable.

First and foremost, I would like to thank my mentor, Dr. Eric Olson, for his never-ending passion for science, for creating such a fun and collaborative lab environment, for his patience and allowing me the freedom to pursue diverse scientific questions. I will always be grateful for the training in his lab and being a part of Olson lab will be one of the most valuable experiences in my life.

I would like to thank Dr. Rhonda Bassel-Duby for facilitating the progress of my thesis research and unlimited support and encouragement for my life in Dallas. I will always be grateful for her help.

I would like to thank my dissertation committee, Drs. Chun-Li Zhang, Joseph Hill, and Ondine Cleaver for their support and guidance over the past several years. Their insights have been critical in completing my projects.

I would like to thank all past and present members of the Olson lab. It was wonderful working with such a dedicated group of scientists. I am particularly grateful to the "reprogramming team": Kunhua Song, Young-Jae Nam, Matthew Dickson, Maria Abad, Gabriela Morales, Hisayuki Hashimoto, Wenduo Ye, Zhaoning Wang. I have been very fortunate to collaborate with them on my research.

Finally, I would like to thank my parents and wife for their unconditional support and love. I would like to thank all my friends in Dallas for having made these years so memorable.

Molecular Regulation of Direct Cardiac Reprogramming

Publication No. _____

Huanyu Zhou, Ph.D.

The University of Texas Southwestern Medical Center at Dallas, 2017

Supervising Professor: Eric N. Olson, Ph.D.

A heart attack (also known as myocardial infarction, MI) happens when the flow of blood to the heart is blocked. A massive heart attack can kill billions of cardiomyocytes. The heart has limited regenerative potential because adult mammalian cardiomyocytes cannot proliferate, therefore lost cardiomyocytes cannot be replaced. This causes permanent heart damage and results in decreased contraction properties to a large portion of the heart muscle. Therapeutic treatments for heart attack patients have improved dramatically over the past decades. However, due to the inability to replenish lost cardiomyocytes, heart failure is still the primary cause of death in the world. Cardiac fibroblasts (CFs) constitute ~50% of the cells in the heart and form scar tissue following heart injury. Reprogramming CFs to induced-cardiomyocytes (iCMs) by forced expression of cardiac specific transcription factors holds promise for enhancing cardiac repair by reducing scar tissue while simultaneously generating new cardiomyocytes. However, low efficiency as well as a lack of understanding of molecular mechanism of the reprogramming

process have significantly hampered its clinical application. The two goals of my PhD study were 1) to optimize the cardiac reprogramming protocol by increasing the efficiency; and 2) to decipher molecular mechanisms of cardiac reprogramming using the information obtained from the optimization process.

To improve the efficiency of reprogramming fibroblasts to iCMs by cardiac transcription factors [Gata4, Hand2, Mef2c, and Tbx5 (GHMT)], we screened 192 protein kinases and discovered that Akt/protein kinase B dramatically accelerates and amplifies this process in three different types of fibroblasts (mouse embryo, adult cardiac, and tail tip). Approximately 50% of the reprogrammed mouse embryo fibroblasts displayed spontaneous beating after 3 weeks of induction by AKT1 plus GHMT (AGHMT). Furthermore, AGHMT evoked a more mature cardiac phenotype for iCMs, as seen by enhanced polynucleation, cellular hypertrophy, gene expression, and metabolic reprogramming. Insulin-like growth factor 1 (IGF1) and phosphoinositol 3-kinase (PI3K) acted upstream of AKT1 whereas the mitochondrial target of rapamycin complex 1 (mTORC1) and forkhead box o3a (Foxo3a) acted downstream of AKT1 to influence fibroblast-to-cardiomyocyte reprogramming. Addition of AGHMT converted 50% of mouse embryo fibroblasts to beating cardiomyocytes. However, only 1% of adult fibroblasts displayed spontaneous beating after three weeks of induction by AGHMT. This indicates that there are "barriers" in adult fibroblasts that hinder cardiac reprogramming. We continued to optimize methods for reprogramming fibroblasts to cardiomyocytes in vitro and in vivo. To identify additional regulators of this reprogramming process, we carried out an unbiased screen of ~1,100 open reading frames (ORFs) encoding transcription factors and cytokines for the ability to enhance reprogramming by AGHMT in adult tail-tip fibroblasts (ATTFs). One of the strongest activators of cardiac reprogramming was Krüppel-Type Zinc-Finger Transcription

Factor 281 (ZNF281). Adding ZNF281 in AGHMT converted ~30% of ATTFs to iCMs which is comparable to AGHMT reprogrammed MEFs. We showed that ZNF281 enhanced cardiac reprogramming by associating with GATA4 on cardiac enhancers and by inhibiting inflammatory signaling, which antagonizes cardiac reprogramming. Our findings not only identify AKT1 and ZNF281 as robust and efficient activators of adult cardiac reprogramming, but also provide new insights into the molecular mechanisms underlying direct cardiac reprogramming.

TABLE OF CONTENTS

PRIOR PUBLICATIONS

Zhou H, Dickson ME, Kim MS, Bassel-Duby R, Olson EN. Akt1/protein kinase B enhances transcriptional reprogramming of fibroblasts to functional cardiomyocytes. *Proc Natl Acad Sci U S A*. 2015 Sep 22;112(38):11864-9. doi:a.10.1073/pnas.1516237112. PubMed PMID: 26354121; PubMed Central PMCID: PMC4586885.

Moon J*, **Zhou H***, Zhang LS, Tan W, Liu Y, Zhang S, Morlock LK, Bao X, Palecek SP, Feng JQ, Williams NS, Amatruda JF, Olson EN, Bassel-Duby R, Lum L. Blockade to pathological remodeling of infarcted heart tissue using a porcupine antagonist. *Proc Natl Acad Sci U S A*. 2017 Feb14;114(7):1649-1654. doi:10.1073/pnas.1621346114. PubMed PMID: 28143939. (* co-first author)

Abad M, Hashimoto H, **Zhou H**, Morales MG, Chen B, Bassel-Duby R, Olson EN. Notch inhibition enhances cardiac reprogramming by increasing MEF2C transcriptional activity. *Stem Cell Reports*. 2017 Mar 14;8(3):548-560. doi: 10.1016/j.stemcr.2017.01.025.

Zhou H, Morales G, Hashimoto H, Dickson ME, Niederstrasser H, Ye W, Min S. Kim, Chen B, Wang Z, Bassel-Duby R, Olson EN. Activation of cardiac enhancers and inhibition of the inflammatory response promotes cardiac reprogramming of adult fibroblasts. (manuscript in preparation)

TABLE OF FIGURES

LIST OF ABBREVIATIONS

AGHMT	Akt1, gata4, hand2, mef2c and tbx5
αMHC	Alpha myosin heavy chain
ATTFS	Adult tail-tip fibroblasts
Ca^{2+}	Ionic calcium
CDNA	Complementary deoxyribonucleic acid
CFS	Cardiac fibroblasts
DEX	Dexamethasone
DNA	Deoxyribonucleic acid
FOXO3A	Forkhead box o3 a
GATA4	Gata binding protein 4
GFP	Green fluorescent protein
GHMT	Gata4, hand2, mef2c and tbx5
GMT	Gata4, mef2c and tbx5
HAND2	Heart- and neural crest derivatives-expressed protein 2
ICMs	Induced-cardiomyocytes
IGF-1	Insulin-like growth factor 1
KO	Knockout
LAD	Left anterior descending coronary artery
MEF2C	Myocyte-specific enhancer factor 2c
MG	Si unit, milligram
MI	Myocardial infarction
mL	Si unit, milliliter
mM	Si unit, millimolar
μM	Si unit, micromolar
mRNA	Messenger ribonucleic acid
mTOR	Mechanistic target of rapamycin
Nab	Nabumetone
nm	Si unit, nanomolar
mM	Si unit, millimeters
ORF	Open reading frame
PCR	Polymerase chain reaction
PI3K	Phosphoinositide 3-kinase
PKB	Protein kinase b
PRC1	Polycomb repressive complex 1
qPCR	Quantitative polymerase chain reaction
RNA	Ribonucleic acid

RPKM	Reads per kilobase per million
TBX5	T-box transcription factor TBX5
TFs	Transcription factors
TGFβ	Transforming growth factor β
UTR	Untranslated region
WT	Wild-type
ZNF281	Zinc finger protein 281

CHAPTER 1. INTRODUCTION

1.1 SOMATIC CELL REPROGRAMMING

A multicellular organism, like the human being, consists of many different cell types such as cardiomyocytes, neurons and fibroblasts, which are differentiated from stem cells during the development process. Once established, the cellular identity of a differentiated cell type is considered to be stable and irreversible, and is maintained by its own regulatory networks that contain a specific combination of regulators, such as epigenetic modifications and transcription factors (TFs). This dogma was challenged by the discovery of MyoD, a skeletal muscle specific TF, that can convert fibroblasts to myoblasts (1). The robust reprogramming ability of MyoD suggested that it is possible to change the cellular identity of a terminally differentiated cell type to another by ectopic expression a single transcription factor.

The cellular reprogramming strategies that bypass normal developmental processes provided a promising approach for obtaining clinically applicable cell types for regenerative medicine. However, most cross lineage reprogramming cannot be achieved by one single factor. MyoD was considered to be a special case until Yamanaka and his colleague showed ectopic expression of four TFs, OCT4, SOX2, KLF4 and c-Myc can convert a fibroblast, a terminally differentiated cell type to an induced pluripotent stem cell (iPSC) in both mice and humans (2, 3). Yamanaka's discovery suggested a combination of factors instead of just one factor is needed to induce a new cell type. This finding opened a door for somatic cell reprogramming. Since then, many different cell types have been reprogrammed, such as neurons (4), hepatocytes (5), and pancreatic cells (6). The field of somatic cell reprogramming by defined factors is still in a nascent stage but has already attracted a lot of attention. Besides the potential benefit of somatic

cell reprogramming for regenerative therapies, disease modeling and drug discovery, it provides a new way to study TF function independent of the physiological environment, and can become a new toolbox to study molecular and developmental biology.

1.2 DIRECT CARDIAC REPROGRAMMING FOR HEART REPAIR

Yamanaka's discovery not only achieved a protocol to generate iPSCs by defined factors but also provided a methodology for somatic cell reprogramming by following these steps: 1) generate a reporter mouse line for a certain cell type; 2) choose a group of candidate factors based on their biological function in a certain cell type; 3) test the ability of pooled candidate factors to induce reprogramming; 4) serial depletions of one factor from the pool to determine the minimal combination of factors that possess the most efficient reprogramming efficiency. Srivastava and colleagues adopted this method to search for a combination of TFs to reprogram mouse fibroblasts to cardiomyocytes (7). They isolated fibroblasts from a cardiac specific αMHC-GFP mouse line and found a pool of cardiac TFs and miRNAs that has the ability to reprogram fibroblasts to induced cardiomyocytes (iCMs). After serial optimization, they found that three cardiac TFs, GATA4, MEF2c and TBX5 (GMT) are sufficient for cardiac reprogramming, albeit at a low efficiency (8). Additionally, our group showed that addition of HAND2 to GMT (GHMT) converts fibroblasts to a more mature cardiomyocyte state than GMT (9). These findings show that cardiac reprogramming is a direct process that bypasses the cardiac progenitor cell stage.

After the initial cardiac reprogramming cocktail was published, the outstanding question became whether this cardiac reprogramming approach can be applied in vivo remained. If achievable, can this approach be used for mammalian adult heart repair? To address those questions, The Srivastava lab and our lab injected retroviruses expressing GMT (8) or GHMT

(9) into the mouse heart after left anterior descending coronary artery (LAD) ligation and showed that non-cardiomyocytes in the injured heart, such as fibroblasts can be reprogrammed to functional cardiomyocytes. In vivo cardiac reprogramming resulted in the iCMs appearing more mature and more closely resembling endogenous cardiomyocytes than seen with in vitro reprgramming. More strikingly, the reduced mouse cardiac functions caused by LAD-ligation was partially restored after injecting the cardiac reprogramming expressing viruses in both studies (8-9). These proof-of-concept studies suggest that the cardiac reprogramming strategy has the potential for heart repair in a clinical setting.

Unlike mouse fibroblasts, neither GMT nor GHMT could reprogram human fibroblasts to iCMs, indicating that additional factors are needed for human iCMs reprogramming. Our lab showed that GHMT plus Myocardin (GHMMT) is sufficient to reprogram human fibroblasts to iCMs. Adding two cardiac miRNAs, miR-1 and miR-133, could further increase the efficiency (10). The Srivastava lab generated another cocktail for human iCM reprogramming that contained GMT plus ESRRG and MESP1. They also showed that adding Myocardin and ZFPM2 could further increase the efficiency (11). The Ieda lab also showed GMT plus Myocardin and MESP1 could reprogram human fibroblasts to iCMs (12). All three cocktails include Myocardin, indicating its vital role in human iCMs reprogramming.

There are several subtypes of cardiomyocytes including atrial, ventricular and pacemaker (PM) cells. Optimal cardiac function relies on all three kinds of cardiomyocytes subtypes. Our lab showed the GHMT-reprogrammed iCMs generate all three major cardiac subtypes and these three subtypes of cardiomyocytes are directly reprogrammed from fibroblasts without going through a progenitor cell intermediate (13). The question remains as to how to induce GHMT-

reprogrammed iCMs to a specific subtype. Optimization of CM subtype-specific reprogramming is still under investigation.

1.3 MOLECULAR REGULATION OF DIRECT CARDIAC REPROGRAMMING

Reprogramming CFs to induced-cardiomyocytes (iCMs) by forced expression of cardiac specific transcription factors holds promise to enhance cardiac repair by reducing scar tissue while simultaneously generating new cardiomyocytes. However, low efficiency as well as lack of understanding the molecular mechanism of the reprogramming process have hampered the potential of clinical application. We and others found that direct cardiac reprogramming can be improved with optimizations of signaling pathways, transcription factors, microRNAs, and epigenetic regulators (15-22) (Figure1-1).

1.3.1 PI3K/Akt signal pathway

The PI3K/Akt signal pathway plays important roles in various aspect of cardiology, including cardiomyocyte survival, energy metabolism and cardiac hypertrophy (14). We recently reported that Akt/protein kinase B dramatically accelerates and amplifies the cardiac reprogramming process in different types of mouse fibroblasts in the presence of GHMT (15). GHMT plus Akt (AGHMT) generated up to 50% iCMs from mouse embryonic fibroblasts, and the iCMs exhibited spontaneous contraction at only 3 weeks. The iCMs formed by AGHMT displayed a higher maturity and functionality, compared to those iCMs generated without Akt as shown by increased cell size, polynucleated iCMs, ratio of Myh6/Myh7 expression and mitochondrial membrane depolarization activity. We also found Akt seems to act in a pathway with insulin-like growth factor 1 (IGF1), phosphoinositol 3-kinase (PI3K), the mitochondrial target of rapamycin complex 1 (mTORC1) and forkhead box o3 (Foxo3a) to boost the cardiac reprogramming process. It will be of eventual interest to determine whether activation of the Akt

signaling pathway enhances cardiac reprogramming of fibroblasts within the context of a myocardial infarct. In this regard, prior studies reported that the 43-amino acid peptide thymosin β4, which activates Akt, enhances cardiac function post-myocardial infarction in the presence of the GMT cardiac reprogramming mixture (8).

1.3.2 Transforming growth factor β (TGFβ) signaling

Transforming growth factor β (TGFβ) signaling is involved in many cellular processes including cell growth, cell differentiation and apoptosis, amd plays critical roles in cardiac development and repair. Multiple groups have discovered that inhibition of TGFβ signaling increased direct conversion of fibroblasts into iCMs (16-19). Ifkovits et al tested several selected small molecules that promote iPSC reprogramming or cardiomyocytes differentiation using an inducible system to overexpress GHMT. They found that treating GHMT mediated reprogrammed cells with SB431542, an Activin, Nodal, and TGFβ inhibitor, led to an increase of 5-fold in iCM yields. A TGFβ specific inhibitor LY364947, which does not inhibit Activin and Nodal pathways, was able to enhance cardiac reprogramming as efficiently as SB431542, indicating SB431542 exerted its effects by inhibiting the TGFβ pathway but not Activin and Nodal pathways (16). Ieda and colleagues reported that miR-133, a cardiac miRNA, promoted cardiac reprogramming by direct repression of Snai1, an important downstream target of the TGFβ pathway signal pathway. Knocking down of Snai1 by shRNA enhanced cardiac gene expression and suppressed fibroblast gene expression in GMT-mediated reprogrammed cells. In contrast, overexpression of Snai1 in GMT-mediated reprogrammed cells maintained fibroblast signatures and inhibited generation of iCMs (17). Zhao et al found that the TGFβ signaling pathway was activated during the first week of cardiac reprogramming and was suppressed in the later stages. They showed that the pro-fibrotic signaling caused by TGFβ signaling pathway

activation is a major barrier of cardiac reprogramming (18). Mohamed et al also identified three TGFβ inhibitors (SB431542, LDN-193189 and dexamethasone) that enhanced cardiac reprogramming by screening a small molecule library that consisted of 5,500 toxicologically tested compounds (19). More strikingly, a TGFβ inhibitor also increased the efficiency of GMT-mediated in vivo cardiac reprogramming (19).

1.3.3 Epigenetic factors

Fibroblasts must overcome epigenetic barriers to become cardiomyocytes during reprogramming, thus epigenetic reprogramming is crucial for this process (20). The epigenetic factors may serve as an inducer or a barrier. Zhou et al. reported that Bmi1 acts as one of the major barriers to direct cardiac reprogramming (21). Bmi1 is a component of Polycomb Repressive Complex 1 (PRC1), which PRC1 represses target gene expression through monoubiquitination of histone H2A at lysine119 ((H2AK119ub). Suppression of Bmi1 enhanced efficiency of cardiac reprogramming. The inhibitory effect of Bmi1 in cardiac reprogramming is mediated through directly binding of the regulatory regions of several cardiogenic genes including Gata4, one of the key factors in the reprogramming cocktail. Knockdown of Bmi1 increased endogenous Gata4 expression and substituted for Gata4 in the reprogramming cocktail during cardiac reprogramming.

1.3.4 Notch signaling pathway

Our lab screened seven small molecule compounds with known roles in iPSC reprogramming and found that the Notch inhibitor DAPT enhanced GHMT or AGHMT mediated cardiac reprogramming (22). The Notch pathway is an evolutionarily conserved signaling pathway that regulates cell-fate specification, differentiation and developmental patterning. It plays an important role in cardiac development by regulating cardiomyocyte

differentiation and proliferation. We showed that DAPT, a classical Notch inhibitor, acted in coordination with Akt1 to increase the acquisition of a mature cardiomyocyte phenotype, demonstrated by increased calcium flux, sarcomere assembly and spontaneous beating. AGHMT plus DAPT generated up to 70% conversion efficiency with 45% of the reprogrammed iCMs exhibiting spontaneous beating. Mechanistically, DAPT increases binding of the transcription factor MEF2C to the promoter regions of cardiac structural genes (22)

1.3.5 ROCK, WNT, FGFs and VEGF signaling

Besides the signaling pathways mentioned above, several other signaling pathways have also been suggested to regulate cardiac reprogramming. Zhao et al showed that ROCK signaling, which plays an important role in fibrosis, was a barrier for cardiac reprogramming. Inhibition of ROCK by Y-27632, increased beating iCMs and decreased the expression of fibrotic genes. Mohamed et al identified a small molecular XAV which inhibits the Wnt signaling pathway to enhance cardiac reprogramming both in vitro and in vivo (19). Yamakawa et al screened several cardiogenic cytokines and found the combination of FGF2, FGF10 and VEGF (FFV) increased the efficiency of GMT-mediated cardiac reprogramming (23). Interestingly, they found that adding Wnt inhibitor IWP4 in FFV further increased the cardiac reprogramming efficiency (23).

1.3.6 Chemical approach for generation of cardiomyocytes

As discussed above, small molecules that modulate signal pathways and epigenetic states are able to enhance transcription factor-mediated direct cardiac reprogramming. A chemical-only approach that does not involve transcription factors to generate cardiomyocytes has been achieved. Cao et al identified an optimal combination of 9 small molecules, A-83-01 (TGF-β inhibitor), AS8351 (Histone demethylase inhibitor), BIX01294 (G9a inhibitor), CHIR99021 (GSK3 inhibitor), JNJ10198409 (PDGF inhibitor), OAC2 (OCT4 expression activator) , SC1

(MAPK/ERK signal pathway inhibitor), SU16F (PDGF receptor β inhibitor) and Y27632 (ROCK inhibitor), to convert human foreskin fibroblasts to cardiac mesoderm cells, which can further differentiate into cardiomyocytes (24). Unlike transcription factors mediated cardiac reprogramming which does not go through a progenitor like state, the existence of a cardiac mesoderm intermediate cell state of this chemical approach indicated it does not occur through direct cardiac reprogramming (24).

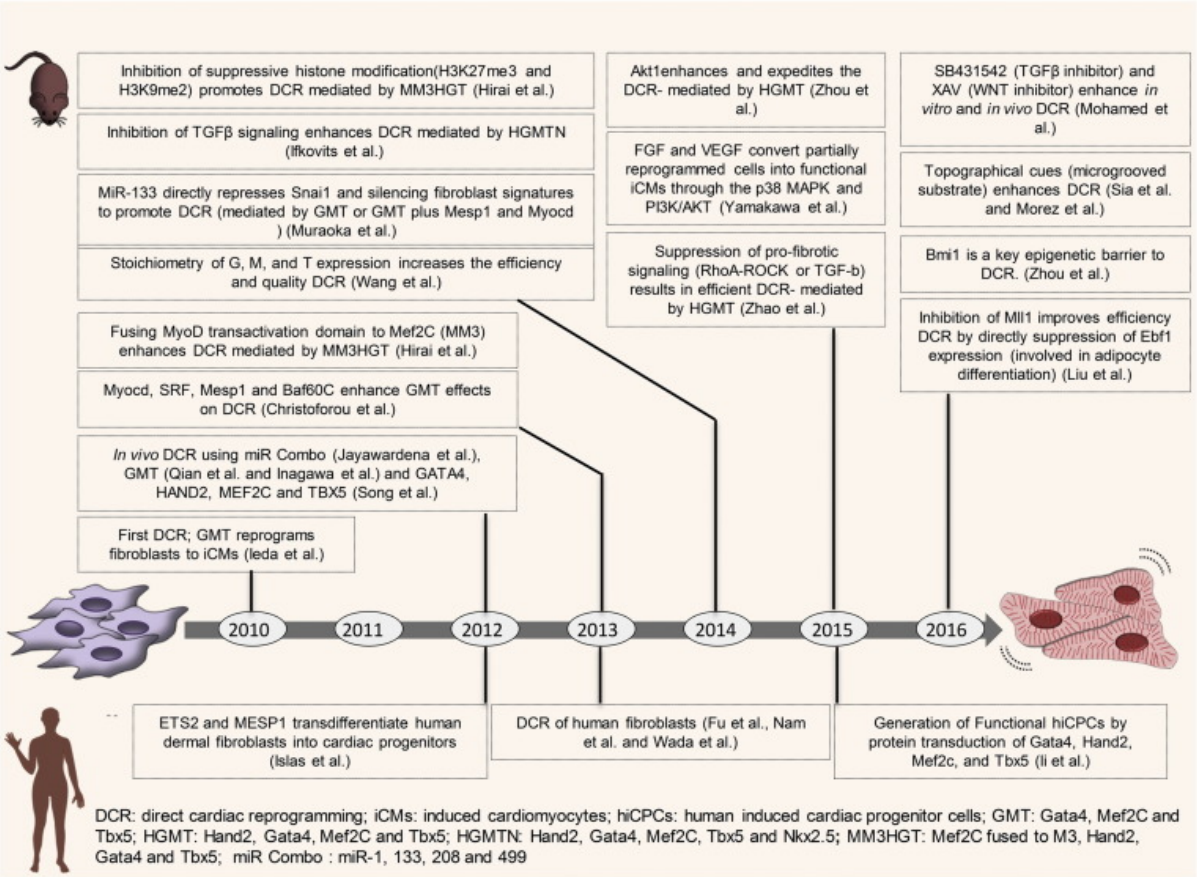

Figure 1-1 Optimization of direct cardiac reprogramming (25).

1.4 REFERENCES

1. Davis, R.L., Weintraub, H., and Lassar, A.B. 1987. Expression of a single transfected cDNA converts fibroblasts to myoblasts. *Cell* 51:987-1000.

2. Takahashi, K., Tanabe, K., Ohnuki, M., Narita, M., Ichisaka, T., Tomoda, K., and Yamanaka, S. 2007. Induction of pluripotent stem cells from adult human fibroblasts by defined factors. *Cell* 131:861-872.

3. Takahashi, K., and Yamanaka, S. 2006. Induction of pluripotent stem cells from mouse embryonic and adult fibroblast cultures by defined factors. *Cell* 126:663-676.

4. Vierbuchen, T., Ostermeier, A., Pang, Z.P., Kokubu, Y., Sudhof, T.C., and Wernig, M. 2010. Direct conversion of fibroblasts to functional neurons by defined factors. *Nature* 463:1035-1041.

5. Pournasr, B., Asghari-Vostikolaee, M.H., and Baharvand, H. 2015. Transcription factor-mediated reprograming of fibroblasts to hepatocyte-like cells. *Eur J Cell Biol* 94:603-610.

6. Wei, R., and Hong, T. 2016. Lineage Reprogramming: A Promising Road for Pancreatic beta Cell Regeneration. *Trends Endocrinol Metab* 27:163-176.

7. Ieda, M., Fu, J.D., Delgado-Olguin, P., Vedantham, V., Hayashi, Y., Bruneau, B.G., and Srivastava, D. 2010. Direct reprogramming of fibroblasts into functional cardiomyocytes by defined factors. *Cell* 142:375-386.

8. Qian, L., Huang, Y., Spencer, C.I., Foley, A., Vedantham, V., Liu, L., Conway, S.J., Fu, J.D., and Srivastava, D. 2012. In vivo reprogramming of murine cardiac fibroblasts into induced cardiomyocytes. *Nature* 485:593-598.

9. Song, K., Nam, Y.J., Luo, X., Qi, X., Tan, W., Huang, G.N., Acharya, A., Smith, C.L., Tallquist, M.D., Neilson, E.G., et al. 2012. Heart repair by reprogramming non-myocytes with cardiac transcription factors. *Nature* 485:599-604.

10. Nam, Y.J., Song, K., Luo, X., Daniel, E., Lambeth, K., West, K., Hill, J.A., DiMaio, J.M., Baker, L.A., Bassel-Duby, R., et al. 2013. Reprogramming of human fibroblasts toward a cardiac fate. *Proc Natl Acad Sci U S A* 110:5588-5593.

11. Fu, J.D., Stone, N.R., Liu, L., Spencer, C.I., Qian, L., Hayashi, Y., Delgado-Olguin, P., Ding, S., Bruneau, B.G., and Srivastava, D. 2013. Direct reprogramming of human fibroblasts toward a cardiomyocyte-like state. *Stem Cell Reports* 1:235-247.

12. Wada, R., Muraoka, N., Inagawa, K., Yamakawa, H., Miyamoto, K., Sadahiro, T., Umei, T., Kaneda, R., Suzuki, T., Kamiya, K., et al. 2013. Induction of human cardiomyocyte-like cells from fibroblasts by defined factors. *Proc Natl Acad Sci U S A* 110:12667-12672.

13. Nam, Y.J., Lubczyk, C., Bhakta, M., Zang, T., Fernandez-Perez, A., McAnally, J., Bassel-Duby, R., Olson, E.N., and Munshi, N.V. 2014. Induction of diverse cardiac cell types by reprogramming fibroblasts with cardiac transcription factors. *Development* 141:4267-4278.

14. Vega, R.B., Konhilas, J.P., Kelly, D.P., and Leinwand, L.A. 2017. Molecular Mechanisms Underlying Cardiac Adaptation to Exercise. *Cell Metab* 25:1012-1026.

15. Zhou, H., Dickson, M.E., Kim, M.S., Bassel-Duby, R., and Olson, E.N. 2015. Akt1/protein kinase B enhances transcriptional reprogramming of fibroblasts to functional cardiomyocytes. *Proc Natl Acad Sci U S A* 112:11864-11869.

16. Ifkovits, J.L., Addis, R.C., Epstein, J.A., and Gearhart, J.D. 2014. Inhibition of TGFbeta signaling increases direct conversion of fibroblasts to induced cardiomyocytes. *PLoS One* 9:e89678.

17. Muraoka, N., Yamakawa, H., Miyamoto, K., Sadahiro, T., Umei, T., Isomi, M., Nakashima, H., Akiyama, M., Wada, R., Inagawa, K., et al. 2014. MiR-133 promotes cardiac reprogramming by directly repressing Snai1 and silencing fibroblast signatures. *EMBO J* 33:1565-1581.

18. Zhao, Y., Londono, P., Cao, Y., Sharpe, E.J., Proenza, C., O'Rourke, R., Jones, K.L., Jeong, M.Y., Walker, L.A., Buttrick, P.M., et al. 2015. High-efficiency reprogramming of fibroblasts into cardiomyocytes requires suppression of pro-fibrotic signalling. *Nat Commun* 6:8243.

19. Mohamed, T.M., Stone, N.R., Berry, E.C., Radzinsky, E., Huang, Y., Pratt, K., Ang, Y.S., Yu, P., Wang, H., Tang, S., et al. 2017. Chemical Enhancement of In Vitro and In Vivo Direct Cardiac Reprogramming. *Circulation* 135:978-995.

20. Liu, Z., Chen, O., Zheng, M., Wang, L., Zhou, Y., Yin, C., Liu, J., and Qian, L. 2016. Re-patterning of H3K27me3, H3K4me3 and DNA methylation during fibroblast conversion into induced cardiomyocytes. *Stem Cell Res* 16:507-518.

21. Zhou, Y., Wang, L., Vaseghi, H.R., Liu, Z., Lu, R., Alimohamadi, S., Yin, C., Fu, J.D., Wang, G.G., Liu, J., et al. 2016. Bmi1 Is a Key Epigenetic Barrier to Direct Cardiac Reprogramming. *Cell Stem Cell* 18:382-395.

22. Abad, M., Hashimoto, H., Zhou, H., Morales, M.G., Chen, B., Bassel-Duby, R., and Olson, E.N. 2017. Notch Inhibition Enhances Cardiac Reprogramming by Increasing MEF2C Transcriptional Activity. *Stem Cell Reports* 8:548-560.

23. Yamakawa, H., Muraoka, N., Miyamoto, K., Sadahiro, T., Isomi, M., Haginiwa, S., Kojima, H., Umei, T., Akiyama, M., Kuishi, Y., et al. 2015. Fibroblast Growth Factors and Vascular Endothelial Growth Factor Promote Cardiac Reprogramming under Defined Conditions. *Stem Cell Reports* 5:1128-1142.

24. Cao, N., Huang, Y., Zheng, J., Spencer, C.I., Zhang, Y., Fu, J.D., Nie, B., Xie, M., Zhang, M., Wang, H., et al. 2016. Conversion of human fibroblasts into functional cardiomyocytes by small molecules. *Science* 352:1216-1220.

25. Srivastava, D., and DeWitt, N. 2016. In Vivo Cellular Reprogramming: The Next Generation. Cell 166:1386-1396.

CHAPTER 2. AKT1/PROTEIN KINASE B ENHANCES TRANSCRIPTIONAL REPROGRAMMING OF FIBROBLASTS TO FUNCTIONAL CARDIOMYOCYTES

The following section titled has been reformatted from its original source in the Proceedings of the National Academy of Sciences, USA [22]. Portions of the data included in this section were contributed by authors Matthew E. Dickson and Min Soo Kim.

2.1 AKT1/PROTEIN KINASE B ENHANCES TRANSCRIPTIONAL REPROGRAMMING OF FIBROBLASTS TO FUNCTIONAL CARDIOMYOCYTES

2.1.1 Abstract

Conversion of fibroblasts to functional cardiomyocytes represents a potential approach for restoring cardiac function following myocardial injury, but the technique thus far has been slow and inefficient. To improve the efficiency of reprogramming fibroblasts to cardiac-like myocytes (iCMs) by cardiac transcription factors (Gata4, Hand2, Mef2c, and Tbx5=GHMT), we screened 192 protein kinases and discovered that Akt/protein kinase B dramatically accelerates and amplifies this process in three different types of fibroblasts (mouse embryo, adult cardiac and tail tip). Approximately 50% of reprogrammed mouse embryo fibroblasts displayed spontaneous beating after three weeks of induction by Akt plus GHMT. Furthermore, addition of Akt1 to GHMT evoked a more mature cardiac phenotype for iCMs, as seen by enhanced polynucleation, cellular hypertrophy, gene expression, and metabolic reprogramming. IGF-1 and PI 3 kinase acted upstream of Akt, whereas mTORC1 and Foxo3a acted downstream of Akt to influence fibroblast-to-cardiomyocyte reprogramming. These findings provide new insights into

the molecular basis of cardiac reprogramming and represent an important step toward further application of this technique.

2.1.2 Introduction

Adult mammalian cardiomyocytes possess limited capacity to proliferate, posing a major barrier to cardiac regeneration following injury (1). Thus, methods to generate induced cardiac-like myocytes (iCMs) by reprogramming fibroblasts with combinations of cardiac transcription factors represent a potential approach for enhancing cardiac repair (2-8). Various cocktails of proteins, microRNAs, and small molecules have been shown to activate cardiac gene expression in fibroblasts (9), confirming original observations made merely five years ago (2). However, the direct lineage conversion technique has been hampered by low efficiency, slow rate of cellular conversion, and production of intermediately reprogrammed or relatively immature iCMs (reviewed in (9)).

We reasoned that altering intracellular signaling pathways via kinase activation might enhance production of iCMs. We therefore screened a library of protein kinases for the potential to enhance reprogramming of fibroblasts to cardiomyocytes by four cardiac transcription factors (Gata4, Hand2, Mef2c, and Tbx5=GHMT). Our unbiased kinase screen revealed that Akt1, also known as protein kinase B (Pkb), dramatically enhances and expedites the formation of iCMs from numerous types of fibroblasts in the presence of GHMT. The iCMs formed by Akt plus GHMT also displayed a mature phenotype compared to those generated without Akt and were responsive to β- adrenoreceptor pharmacologic modulation, polynucleated, and hypertrophic. Akt appears to act in a pathway with insulin-like growth factor 1 (IGF11), phosphoinositol 3-

kinase (PI3K), the mitochondrial target of rapamycin complex 1 (mTORC1) and forkhead box o3 (Foxo3a) to boost the cardiac reprogramming process.

2.1.3 Materials and Methods

2.1.3.1 Mice

All experiments involving animals were approved by the Institutional Animal Care and Use Committee at the University of Texas Southwestern Medical Center.

2.1.3.2 Cell Culture

TTFs, CFs, and MEFs were prepared as described (7,15). MEFs were isolated at E13.5 whereas TTFs and CFs were isolated at 6-10 weeks of age. Retroviral transduction and cellular reprogramming were performed as described (7). Small molecule treatments were utilized either throughout the reprogramming process (20 μM LY294002 = LY from Sigma, 5 nM rapamycin = Rap from Sigma, 10 μM CHIR99021 = CHIR from Selleck Chemicals, 5 μM BIO from Sigma, 300 ng/mL IGF1R3 = Igf1 from Sigma) or at the indicated times (10 μM isoproterenol = Iso from Sigma, 10 μM metoprolol tartrate = Met from Sigma, 20 nM tetramethylrhodamine methyl ester = TMRM from Invitrogen).

2.1.3.3 Generation of Retroviruses

Retroviruses were produced and used analogously to prior description (7,15). The Myristoylated Kinase Library was obtained from Addgene (Cambridge, MA) and contained pWZL vectors with the individual myristoylated, FLAG-tagged inserts.

2.1.3.4 qPCR, Western Blot Analyses, Immunocytochemistry, Flow Cytometry, Beating Cell Analyses, Calcium Transient Measurements, and Cell Size Measurements

These experiments were performed as previously described (7), with the exceptions of beating cell analyses, calcium transient measurements, and cell size measurements. Beating cell analyses and calcium transient measurements were normalized to the initially plated number of fibroblasts. Beating cell analyses were performed by light microscopy at room temperature after retroviral treatment of TTFs, CFs, and MEFs at the indicated time points. Three to nine high-power fields of view were randomly selected for each well, video recorded for three minutes (maintaining the same shutter speed), manually quantified, and averaged to provide an individual replicate. Responses to isoproterenol ± metoprolol tartrate were assessed in similar fashion except that they were each acquired for two minutes starting one minute after addition of the indicated compounds. Calcium transient measurements were performed by fluorescence microscopy at room temperature one week after retroviral treatment of αMHC-Cre/Rosa26A-Flox-Stop-Flox-Gcamp3 MEFs. Three high-power fields of view were randomly selected for each well, video recorded for three minutes (maintaining the same shutter speed of 1.9 seconds), manually quantified, and averaged to yield an individual replicate. Cell size measurements used manually-drawn contours of αMHC- GFP positive iCMs where, as above, three randomly selected fields of view from each well were averaged to provide an individual replicate.

2.1.3.5 Proliferation and Apoptosis Assays

Cells were harvested at the indicated time points and assayed according to manufacturer recommendations using the Click-iT® EdU Alexa Fluor® 647 Flow Cytometry

Assay Kit or the APO-BrdU™ TUNEL Assay Kit (both from Life Technologies, Grand Island, NY).

2.1.3.6 Cell Metabolism Experiments

MEFs were analyzed a week after induction using manufacturer recommendations with XFe Cell Mito Stress Test kits (Seahorse Bioscience, North Billerica, MA). Experiments were normalized to input cell number and used the following drug concentrations within the above test kits: 1 μM oligomycin, 1 μM carbonyl cyanide-4-(trifluoromethoxy) phenylhydrazone (FCCP), or 0.1 μM rotenone.

2.1.3.7 Differential Gene Expression Analysis

We performed RNA-Seq using the Next Generation Sequencing Core at the University of Texas Southwestern Medical Center. Three micrograms of DNAse-treated RNA per replicate were prepared using the TruSeq Stranded LT Kit from Illumina. Samples were then PCR amplified and purified with Ampure XP beads before sequencing on a HiSeq2500 instrument (Illumina, Inc., San Diego, CA). All procedures were carried out according to manufacturer protocols. Quality assessment of the RNA-Seq data was done using NGS-QC-Toolkit (16). Reads with mean phred quality scores of less than 20 were removed from further analysis. Quality filtered reads were then aligned to the mouse reference genome GRCm38 (mm10) using the Bowtie2 (v 2.0.6) aligner (17). Only uniquely mapped reads were kept for further downstream analysis. Differential gene expression analysis was done using the R package DESeq (v 1.10.1) (18) following the protocols outlined in (19). Read counts were normalized by taking the median of each gene count across samples and dividing each sample gene count by the relative ratio of library sizes between the calculated median and sample size. The averaged

normalized expressions values of the triplicate samples were used to calculate fold change and p-values. Cutoff values of fold change greater than two and p- value less than 0.01 were then used to select for differentially expressed genes between sample group comparisons. Our results are archived using the GEO accession number GSE68509.

2.1.3.8 Pathway Enrichment Analysis

Significant pathway enrichment analysis was performed using Ingenuity Pathways Analysis (Ingenuity® Systems, Redwood City, CA). Differentially expressed genes from the RNA expression data are associated with a biological function supported by at least one publication in the Ingenuity® Pathways Knowledge Base. Fisher's exact test is then used to calculate the p-value and determine the probability that each biological function is enriched in the dataset due to chance alone. Statistically significant biological pathways were then identified by selection for pathways with p-values less than 0.05. DAVID gene functional annotation and classification tool (20) was used to annotate the list of differentially expressed genes with respective Gene Ontology terms and perform GO enrichment analysis for molecular and biological functional categories. Functional Gene Ontology groups were selected for significance by using a p-value cutoff of 1%.

2.1.3.9 Statistical Analyses

All in vitro data are presented as mean with S.E.M. and have N=3 per group (except Figure 2-3e with N=6 per group, Figure 2-4c-d with N=2 per group, and Figure 2-4e/g as indicated). P- values were calculated with either unpaired/two-way t-test or one-way ANOVA, as appropriate, except in time-course analyses where we utilized two-way ANOVA. All statistical analyses were run using the GraphPad Prism 6 software package (GraphPad Software, Inc., La

Jolla, CA). $P<0.05$ was considered significant in all cases after corrections were made for multiple pairwise comparisons.

2.1.4 Results

2.1.4.1 Akt enhances GHMT-mediated cardiac reprogramming

Previously, we established a cardiac reprogramming assay by expressing the cardiac transcription factors, GHMT, in mouse tail tip fibroblasts (TTFs) and cardiac fibroblasts (CFs) (7). With the goal of improving the efficiency and rate of reprogramming, we screened a myristoylated kinase expression library for individual kinases that might augment the generation of functional iCMs by GHMT. After 7 days of TTF induction with retrovirally-expressed GHMT plus either GFP or each of the 192 kinases in the library, we harvested RNA and quantified expression of the cardiac markers, Myh6 and Actc1 (Figure 2-1A). Our results showed that over-expression of Akt1 or Akt3 specifically augmented expression of these cardiac markers (Figure 2-1B). Akt2 was not present in this library. We confirmed these findings using a different Akt1 expression cassette (pMxs- MyrAkt1) that directed robust expression of active phospho-Akt1 (Figure 2-7A) and used this vector for all subsequent experiments. Western blot analysis of MEFs isolated from transgenic mice harboring a GFP transgene controlled by the cardiac-specific αMHC promoter confirmed that addition of Akt1 to GHMT enhanced expression of endogenous cardiac markers as well as the αMHC-GFP reporter (Figure 2-1C). Notably, neither Akt1 alone nor a kinase-dead (KD) form of Akt1 was able to induce expression of cardiac markers. Akt1 and Akt2 stimulated cardiac transcript expression comparably in the transdifferentiation assay, whereas the KD mutant form of Akt1 abrogated the stimulatory activity on GHMT (Figure 2-1D). We thus focused on Akt1 for subsequent experiments.

To further monitor the effect of Akt1 on GHMT-mediated cardiac reprogramming of fibroblasts, we isolated mouse embryonic fibroblasts (MEFs), TTFs, and CFs from αMHC-GFP transgenic mice. We observed that the addition of Akt to GHMT (AGHMT) dramatically enhanced the number of iCMs, detected by staining for GFP and cardiac troponin T (cTnT in red, GFP in green, Figure 2-2A-C) or α-actinin (Figure 2-2D-F). A subset of these iCMs showed characteristic striations indicative of sarcomere formation a week after induction (Figure 2-2G for MEFs, Figure 2-2H for CFs,) or after two weeks in the case of TTFs (Figure 2-2I), whereas no sarcomere formation was seen with iCMs formed by GHMT alone at these time points. Using flow cytometry after expression of AGHMT in MEFs isolated from αMHC-GFP mice, we detected a dramatic increase in the percentage of cells positive for endogenous and exogenous cardiac markers compared with GHMT treatment (Figure 2-7 A and D). The percentage of positive cells is noteworthy when considering that the statistical likelihood of an individual fibroblast taking up the four-to- five separate retroviruses encoding the transdifferentiation factors would be less than 100%. Similar experiments in CFs (Figure 2-7 B and E) and TTFs (Figure 2-7 C and F) yielded compatible results after 7 days of transdifferentiation, although the absolute percentage of positive cells was not as pronounced as in MEFs. We further observed an increase in the percentage of α-actinin-positive cells by flow cytometry when adding Akt1 to GHMT in these different types of fibroblasts (data not shown).

2.1.4.2 Akt1 enhances calcium flux and spontaneous cell beating in response to GHMT

To examine the potential influence of Akt on calcium flux and spontaneous cell beating in response to GHMT, we used a conditionally active modified GFP reporter system (αMHC-Cre/Rosa26A-Flox-Stop-Flox-GCamp3 MEFs) for live cell imaging of spontaneous

cellular calcium flux as detected by autofluorescence (Figure 2-8). AGHMT- treated MEFs had greater calcium flux following a week of transdifferentiation than GHMT-treated MEFs, and a majority of the AGHMT-treated cells exhibited calcium flux with many cells seemingly firing in unison (Figure 2-3A).

Spontaneous beating represents a phenotype of mature cardiomyocytes, requiring functional sarcomeres and calcium cycling machinery, rather than spontaneous intracellular calcium flux alone. We observed a similar increase in spontaneous beating of MEFs (Figure 2-3B; there were very rare spontaneously beating cells only at 20 days in the GHMT treatment group), CFs (Figure 2-3C; 2 weeks after induction), and TTFs (Figure 2-3D; 3 weeks after induction) upon addition of Akt1 to GHMT. We observed no beating cells in CFs or TTFs following 2 or 3 weeks of GHMT induction, respectively, and we observed no beating cells with Empty Vector or Akt1 alone in any fibroblast cell type.

To further characterize the properties of AGHMT-mediated iCMs, we tested the effects of adrenergic agonists and antagonists on AGHMT-induced MEFs 21 days after induction (Fig. 3E). AGHMT-mediated iCMs were responsive to pharmacologic modulation of β-adrenoreceptor activity. Although more difficult to quantify, it also appeared that altering β-adrenoreceptor activity had an effect on iCM inotropy.

We noted that numerous AGHMT-treated iCMs became binucleate (Figure 2-4A and B, E and F, Figure 2-10A and S4B) or multinucleate (3 or more nuclei, Figure 2-4D and G, Figure 2-10C) within 3 weeks, whereas such cells were observed only rarely following induction with GHMT. We therefore examined whether AGHMT-induced iCMs displayed other features of

mature cardiomyocytes, including an altered metabolic profile, increased ratio of Myh6:Myh7 expression, increased cell size, and mitochondrial membrane depolarization activity. AGHMT treatment of fibroblasts resulted in an approximate doubling of iCM size after three weeks of induction relative to GHMT treatment (Figure 2-4D and H, Fig. S4D). Akt1 added to GHMT treatment also increased the ratio of Myh6:Myh7 RNA expression as assessed by qPCR (Figure 2-10E).

Metabolic analysis showed that AGHMT-treated MEFs had higher baseline oxygen utilization per cell a week after induction than non-Akt1 treated cells and greater possible maximal oxygen consumption than other tested cells (Figure 2-4K). This experiment measured oxygen consumption rate normalized to input cell number at baseline and in the presence of several compounds that counteract various stages of oxidative phosphorylation: oligomycin inhibits ATP synthase by blocking its F0 subunit (proton channel) and hence severely limits oxygen utilization, FCCP uncouples the hydrogen ion gradient needed for ATP synthesis and hence maximizes oxygen utilization, and rotenone prevents electron transfer from Complex I to ubiquinone within the electron transport chain and also minimizes oxygen utilization. The lack of difference between oligomycin and rotenone treatments suggests that the metabolic effects of Akt1 are not specific to a component of the electron transport chain but rather represent a more general metabolic phenotype. Moreover, addition of Akt1 to GHMT increased mitochondrial membrane depolarization in MEFs and CFs as determined by use of a membrane permeable dye that is taken up by active mitochondria (Figure 2-4I and J). All of these measurements, in addition to the above qualitative change in cellular inotropy with isoproterenol, corresponded to a more mature iCM phenotype after AGHMT treatment.

We performed RNA-Seq using either isolated adult mouse ventricular cardiomyocytes (CMs) or MEFs treated for three weeks with empty vector, GHMT (iCMs cell sorted using αMHC-GFP before RNA-Seq), or AGHMT (iCMs cell sorted using αMHC-GFP before RNA-Seq, Table S1). These data showed that global RNA expression profiles of iCMs formed with AGHMT were more similar to mature CMs than those formed with GHMT (Figure 2-5A, Figure 2-8A). Some specific cardiac markers of interest that displayed increased expression in AGHMT relative to GHMT iCMs are shown in Figure 5B. It appeared that the effects of Akt1 were mediated predominantly by increases in cardiac marker expression (Figure 2-8B and C). Using a two-fold cutoff and $p<0.01$ threshold for inclusion, ~1600 markers differed between CMs and MEFs treated with Empty Vector. Restricting analysis to these ~1600 markers and only counting those that changed expression in the same direction as CMs, ~800 changed for AGHMT (vs. Empty Vector) while only ~350 changed for GHMT (vs. Empty Vector, Figure 2-5C). This suggests that AGHMT iCMs are more similar to mature CMs than GHMT iCMs. Notably, neither AGHMT nor GHMT iCMs had very many of these ~1600 markers that changed in ways predicted to make them less like mature CMs (i.e. – more like MEFs than like mature CMs). Pathway analyses showed changes in marker expression patterns between GHMT and AGHMT iCMs indicative of a shift toward a more cardiomyocyte- like phenotype with AGHMT: changes in mitochondrial function, cellular metabolism, sarcomere/cytoskeleton organization, and β-adrenoreceptor function to name a few (Figure 2-5D).

2.1.4.3 Analysis of the mechanism of Akt1-dependent reprogramming

To begin to define the molecular mechanism whereby Akt signaling enhanced reprogramming by GHMT, we examined whether Akt1 might function by enhancing GHMT

expression. Measurement of GHMT expression by RT-PCR (Fig. S5B) or Western blot analysis (Figure 2-6A) showed Akt did not increase expression of these reprogramming factors.

We next tested the impact of multiple components of intracellular signaling pathways involving Akt on the reprogramming process. MEFs treated with Igf1, an upstream activator of Akt signaling, had higher rates of conversion to iCMs than GHMT- treated cells as assessed by flow cytometry (Figure 2-6A). Conversely, pharmacological inhibition with LY294002 of Pi3 kinase (PI3K), which signals from the IGF1 receptor to Akt, reduced the formation of iCMs. This effect was attenuated by constitutively active Akt1 (Figure 2-6B-C).

We also analyzed the potential influence of downstream mediators of Akt1 signaling on cardiac reprogramming. Pharmacologic inhibition of mTORC1 and/or genetic addition of Foxo3a in GHMT-treated MEFs impaired cardiac reprogramming by AGHMT (Figure 2-6D-E). These results suggest that mTORC1 and Foxo3a act as downstream mediators of Akt1 in transdifferentiation. Pharmacologic inhibition of glycogen synthase kinase 3 (Gsk3), an antagonist of Akt signaling, did not alter cardiac gene expression in a way supporting its function downstream of Akt1 in cardiac reprogramming.

Since Akt could potentially enhance transdifferentiation by increasing proliferation of iCMs, we performed dual EdU/cTnT staining and analyzed MEFs using flow cytometry after a week of induction (Fig. S5D and E). The results showed reduced proliferation of both MEFs and iCMs treated with GHMT or AGHMT. The reduction in proliferation when comparing GHMT- or AGHMT-treated MEFs to iCMs indicated that iCMs likely quickly exit the cell cycle during the reprogramming process. It is possible that AGHMT-treated cells do so

more quickly, as shown by the significantly lower percentage of EdU+ AGHMT-treated iCMs after a week of induction. To test whether Akt alters apoptosis levels after transdifferentiation, we performed BrdU staining of MEFs a week after induction but observed no difference in apoptosis between cells treated with GHMT and AGHMT.

We interpret the above results to indicate a mechanism of action for Akt1 whereby IGF1 signals (likely through the IGF receptor) via PI3K to Akt, and then active pathways downstream of Akt that are involved in iCM formation include mTORC1 and Foxo3a (Figure 2-6F). Other pathways identified by RNA-Seq analysis (Figure 2-5) may play additional roles in this process.

2.1.5 Discussion

We show that addition of Akt1 significantly boosts iCM formation in vitro compared with GHMT treatment alone. These effects were validated by a variety of biochemical, structural, and functional assays, suggesting a robust effect overall. We noted large increases in number of cells with calcium flux and beating upon treatment with AGHMT, and the resultant cells were both hypertrophic and responsive to β-adrenoreceptor pharmacologic manipulation. AGHMT-treated cells also displayed changes in metabolism, mitochondria, morphology, multi-/bi-nucleation, and gene expression corresponding to a more mature cardiomyocyte phenotype than GHMT-treated cells (maturation criteria were reviewed recently for engineered iCMs (10). We additionally found that some fibroblast genes have enhanced expression in AGHMT-reprogrammed cells. The functional significance of this finding remains unclear. Akt appears to signal through a pathway involving IGF1, PI3K, mTORC1, and Foxo3a to enhance reprogramming (Figure 2-6F). These results represent a significant advance over existing

techniques in producing iCMs via direct lineage conversion, which until now have been largely limited by inefficiency of the reprogramming process. This is the first time, to our knowledge, that polynucleate iCMs have been described by direct lineage conversion, and addition of Akt1 to GHMT treatment significantly increases production of these cells. It will be of eventual interest to determine whether activation of the Akt signaling pathway enhances cardiac reprogramming of fibroblasts within the context of a myocardial infarct. In this regard, prior studies (6,11) reported that the 43 amino acid peptide thymosin β4, which activates Akt, enhances cardiac function post-myocardial infarction in the presence of a GMT (Gata4, Mef2c, and Tbx5) cardiac reprogramming cocktail (6).

In comparison to adult fibroblasts, embryonic fibroblasts are easier to reprogram to other cell types. Interestingly, we show that adult CFs are more amenable to reprogramming into cardiomyocytes than adult TTFs. This could be due to the fact that CFs already express GHMT factors (21), although not at levels sufficient to turn CFs into cardiomyocytes.

We enhanced GHMT-mediated iCM formation by addition of IGF1, which is an activator of the Akt signaling pathway via PI3K. However, reprogramming with GHMT+IGF1 was less efficient than with AGHMT (Figure 2-6A). We attribute this to the fact that IGF1 is not the only factor controlling the Akt signaling pathway. Furthermore, overexpression of constitutively activated Akt in the reprogramming assay provides a more potent effect than activating endogenous Akt by IGF1. Downstream of Akt1 there are many potential effectors. While at least some signaling occurs through mTORC1 and Foxo3a, there does not appear to be significant signaling through Gsk3. That the mechanism of Akt1 involves mTOR and FoxO is intriguing given their roles in regulating mitochondrial metabolism, muscle development, and gene

expression; in fact, these are some of the key changes that we have documented in response to adding Akt1 to our reprogramming cocktail. Moreover, our RNA-seq analysis confirmed expression changes for markers involved with mitochondrial metabolism, sarcomeres/cytoskeletal components, and β-adrenergic signaling. The realization that Akt signaling enhances the reprogramming process raises possibilities for further augmenting this process through pharmacologic manipulation of aspects of this pathway.

Cardiomyocyte bi- and multi-nucleation, as observed in response to reprogramming with AGHMT, results from progression through S-phase of the cell cycle without subsequent cytokinesis. It is interesting that Akt has been implicated in both cardiac hyperplasia and hypertrophy depending on the specific context (12,13). It is conceivable that Akt simultaneously stimulates hypertrophy, DNA replication, and cellular senescence similarly to development of mature/polynucleate mammalian cardiomyocytes.

The ability to use iCMs for therapeutic purposes in humans with various cardiomyopathies remains a long-term goal of cardiac reprogramming research, but technical boundaries must be crossed before this is feasible. The concern that iCMs are formed with low efficiency using direct lineage conversion can be reduced by the gains imparted by addition of Akt to the reprogramming cocktail. There remains a concern that gene delivery by integrating retroviruses may not be compatible with future clinical use of this technology, though this concern is not insurmountable.

2.1.6 Figures

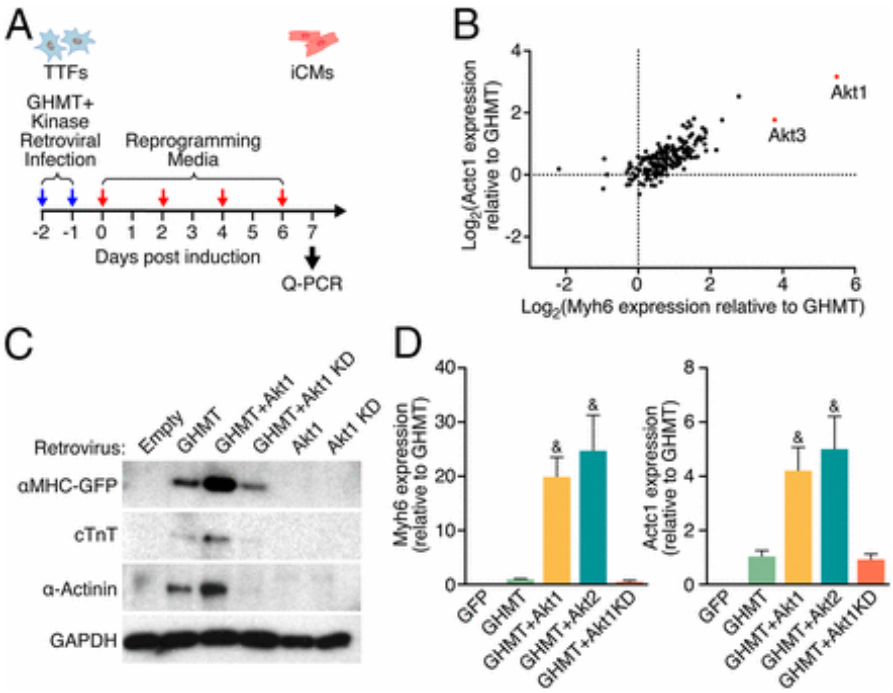

Figure 2-1 A kinase screen identifies Akt as an enhancer of cardiac reprogramming by GHMT.

(A) Protocol for reprogramming and the kinase library screen. (B) Transcript levels measured by qPCR 7 d after TTF induction with GHMT plus either GFP or one of the retrovirally expressed kinases. This log–log plot is normalized to expression with GHMT+GFP and shows that Akt1 and Akt3 caused the greatest increases in cardiac marker expression. (C) Detection of cardiac markers by Western blot of protein lysates from αMHC-GFP transgenic MEFs a week after induction with the indicated retroviruses. KD, kinase dead. (D) Transcript levels of Myh6 and Actc1 were increased a week after induction by adding Akt1 or Akt2 to GHMT in TTFs. &P < 0.05 vs. all others unless also labeled with "&."

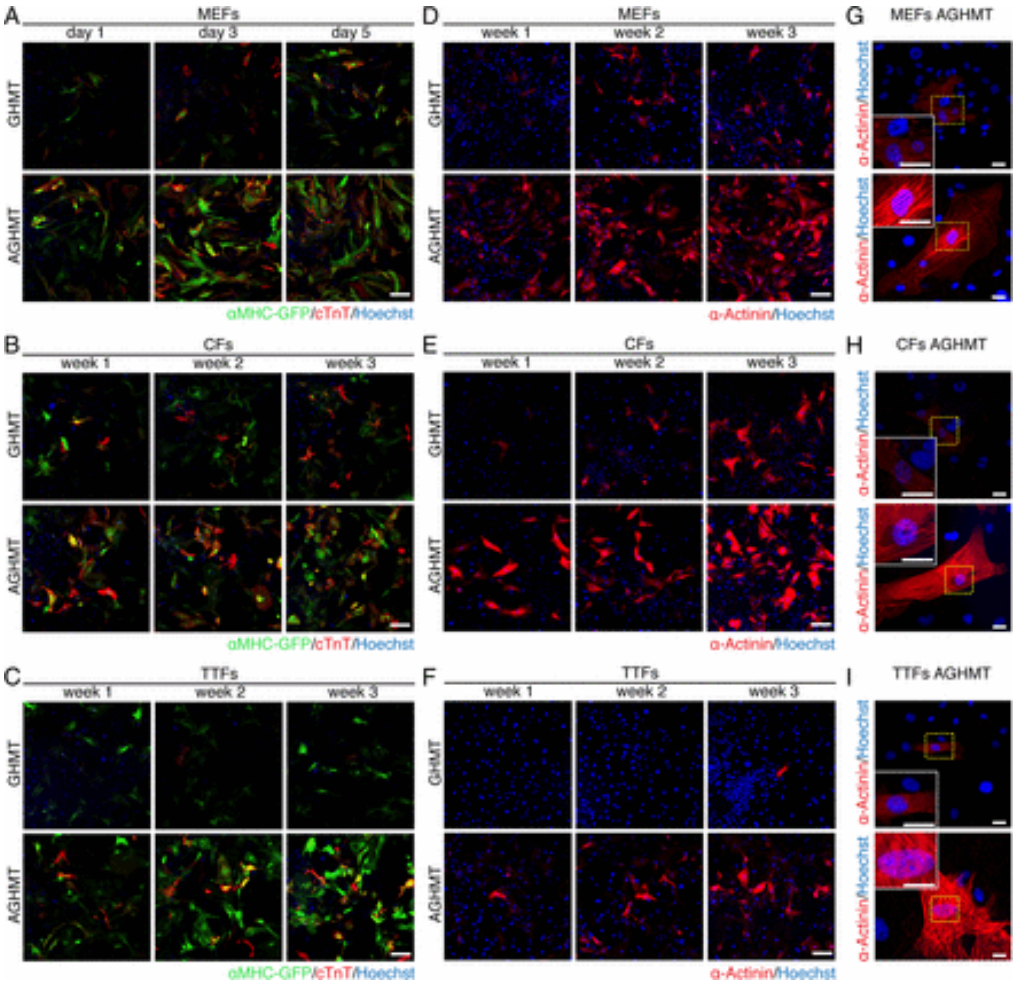

Figure 2-2 Akt enhances cardiac reprogramming by GHMT.

(A–C) Immunocytochemistry of αMHC-GFP transgenic MEFs, CFs, and TTFs, respectively, at the indicated times showed more cells positive for GFP (green) and cTnT (red) with AGHMT compared with GHMT. (Scale bars: 200 μm.) (D–F) α-Actinin immunocytochemistry (red) of MEFs, CFs, and TTFs, respectively, at the indicated times showed enhanced reprogramming upon addition of Akt1 to GHMT. (Scale bars: 200 μm.) (G–I) α-Actinin staining of MEFs, CFs, and TTFs showed striations suggestive of sarcomere formation by 7 d of induction in AGHMT but not GHMT (two weeks for TTFs). (Scale bars: 25 μm.)

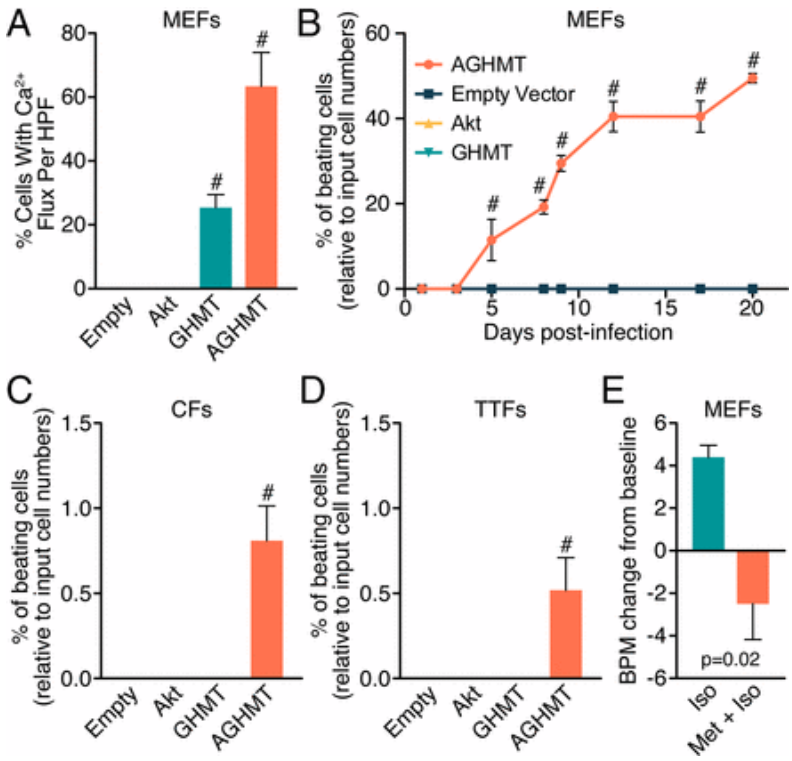

Figure 2-3 Akt1 promotes spontaneous calcium flux and cellular beating in iCMs.

Whole mounts of E18.5 diaphragm muscles were double-stained with Texas red α-bungarotoxin to label postsynaptic AChRs and an antibody against syntaxin to label presynaptic nerves. In both WT and KO muscles, presynaptic nerve terminals formed in juxtaposition with postsynaptic AChR clusters (B). However, there were increased nerve branching and defasciculation in the KO diaphragm compared with the WT (A). AChR clusters also occupied a broader area in the central region of the KO diaphragm. [Scale bars, 400 μm (A), 20 μm (B).

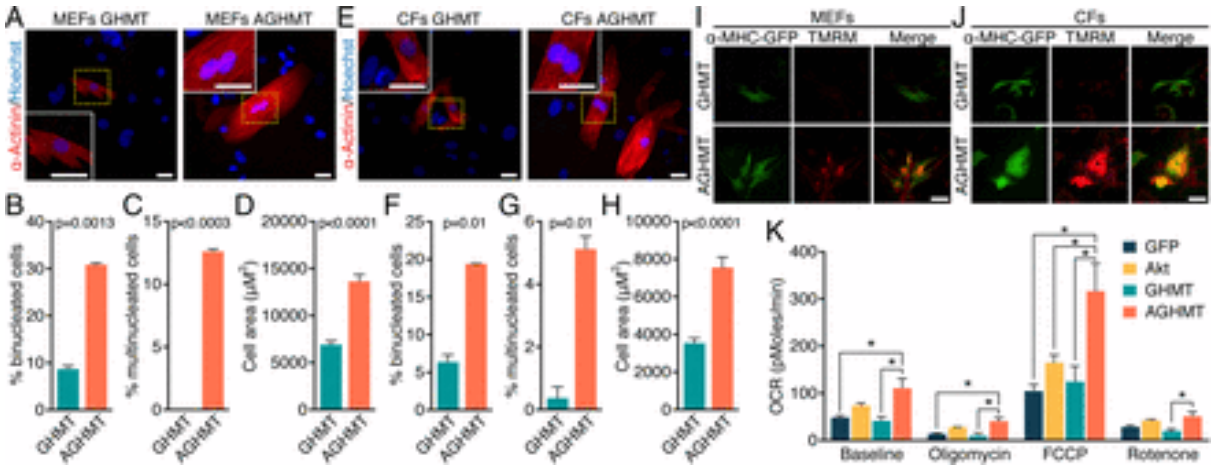

Figure 2-4 Addition of Akt1 to GHMT stimulates maturation of iCMs.

(A) Examples of miniature end-plate potential (mEPP) traces obtained from 1-min continuous recording (superimposed traces are shown; 60×, 1-s). mEPP frequencies were significantly increased in E18.5 KO mice compared with WT. (B) Quantification of mEPP frequencies and amplitudes. Frequency: KO (27.99 ± 7.73 events per min, n = 22 cells), WT (1.15 ± 0.13 events per min, n = 13 cells), *P < 0.05; mEPP amplitude (no statistical difference): KO (2.4 ± 0.3 mV, n = 22 cells), WT (2.04 ± 0.3 mV, n = 13 cells). (C) Sample traces of end-plate potentials. (D) Quantification of EPP amplitudes (no statistical difference): WT (14 ± 1.44 mV, n = 9 cells) and KO (16.46 ± 1.01 mV, n = 16 cells). Statistical data are represented as mean ± SEM. (E) Traces of muscle action potentials are comparable in WT and KO. The arrowhead indicates a contraction artifact, which was not observed in KO muscles due to their paralysis.

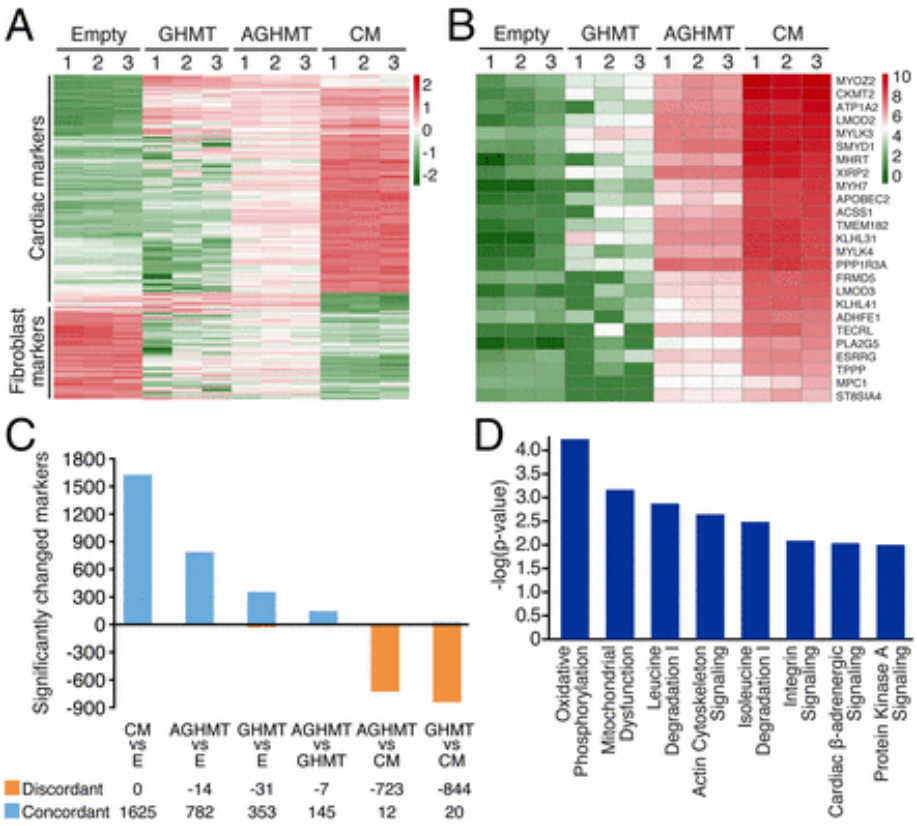

Figure 2-5 Comprehensive expression analysis by RNA-Seq shows that AGHMT iCMs are more similar to adult mouse ventricular cardiomyocytes than GHMT iCMs.

(A and B) Heatmaps of RNA expression data illustrating differentially expressed markers in empty vector, GHMT, AGHMT, and CMs. Red indicates up-regulated markers, and green indicates down-regulated markers. (C) Restricting analysis to the 1,625 markers that differed between CMs and MEFs and only counting those that changed expression in the same direction as CMs, 782 changed for AGHMT whereas only 353 changed for GHMT. These findings suggest that AGHMT iCMs are more similar to mature CMs than GHMT iCMs. Notably, AGHMT and GHMT iCMs had only 14 and 31 markers, respectively, that changed to look more like MEFs. (D) Analysis showed expression changes in key pathways between GHMT and AGHMT iCMs, indicating a more cardiomyocyte-like phenotype with AGHMT.

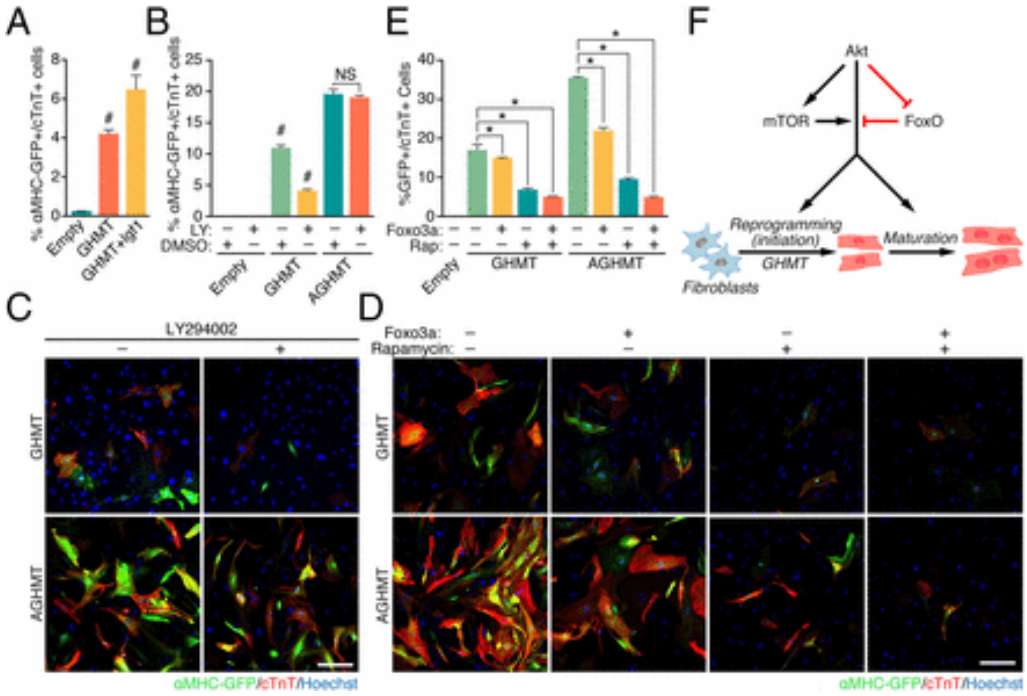

Figure 2-6 Akt1 enhancement of GHMT-mediated reprogramming relies on signaling through IGF1, PI3K, mTORC1, and Foxo3a.

(A) IGF1 (300 ng/mL) enhanced the proportion of MEFs expressing cardiac markers detected by flow cytometry a week after induction. (B and C) A similar experiment using pharmacologic inhibition of PI3K activity ± genetic rescue by Akt1 suggested that PI3K activity may stimulate GHMT-mediated transdifferentiation into iCMs. LY, LY294002 (PI3K antagonist). (Scale bar: 200 μm.) (D and E) After 7 d induction of MEFs, we also found that pharmacologic inhibition of mTORC1 and/or genetic addition of Foxo3a incrementally attenuated formation of iCMs (rapamycin, mTORC1 antagonist). (Scale bar: 200 μm.) Upon treatment with both rapamycin and Foxo3a, residual formation of iCMs was equal when comparing GHMT and AGHMT treatments. (F) Proposed mechanism of action by which Akt1 enhances GHMT-mediated formation of induced cardiac-like myocytes. *$P < 0.05$; #$P < 0.05$ vs. all others.

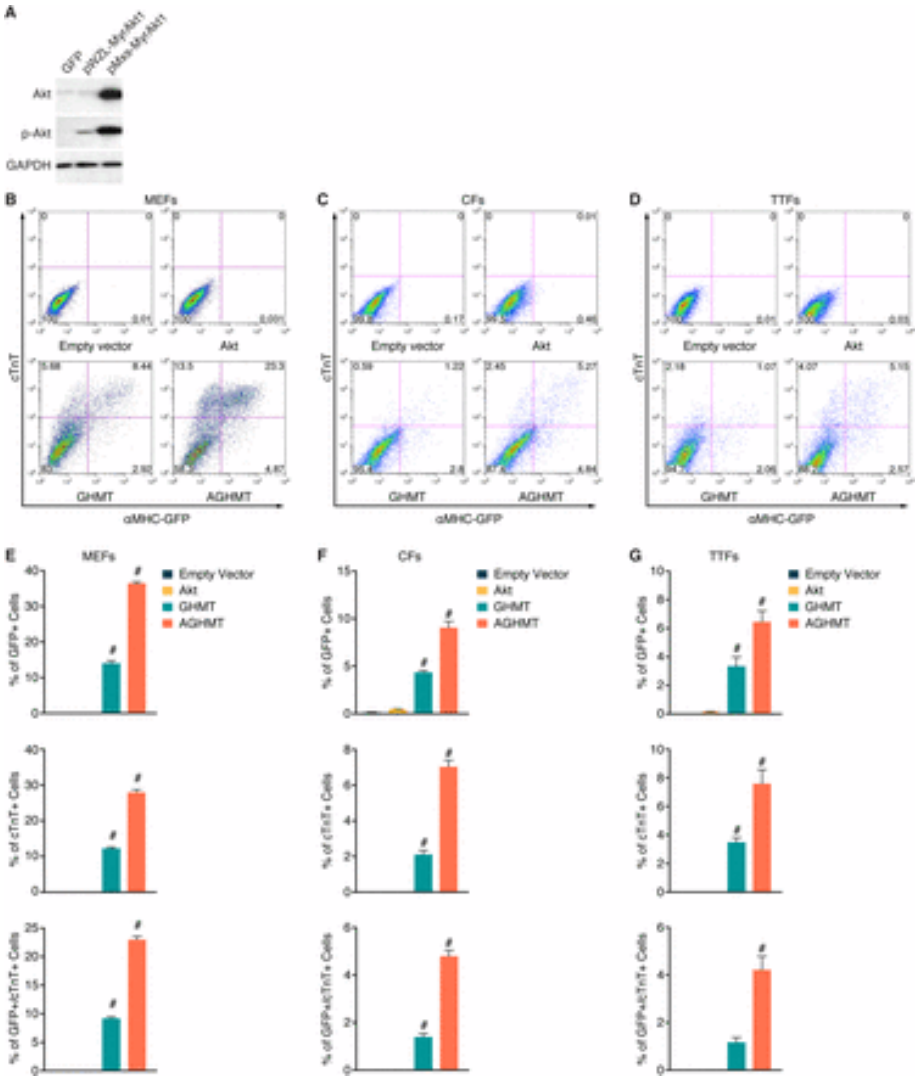

Figure 2-7 Akt enhances cardiac reprogramming by GHMT.

(A) Western blot of Akt and phospho-Akt in TTFs 7 d after infection with the indicated retroviral Akt expression cassettes. (B–D) Representative flow cytometry plot and (E–G) analyses of αMHC-GFP+ and cTnT+ cells in MEFs, CFs, or TTFs, after infection with control, Akt, GHMT, or AGHMT retrovirus at indicated times (5 d for MEFs, 1 wk for CFs and TTFs). #P < 0.05 vs. all others.

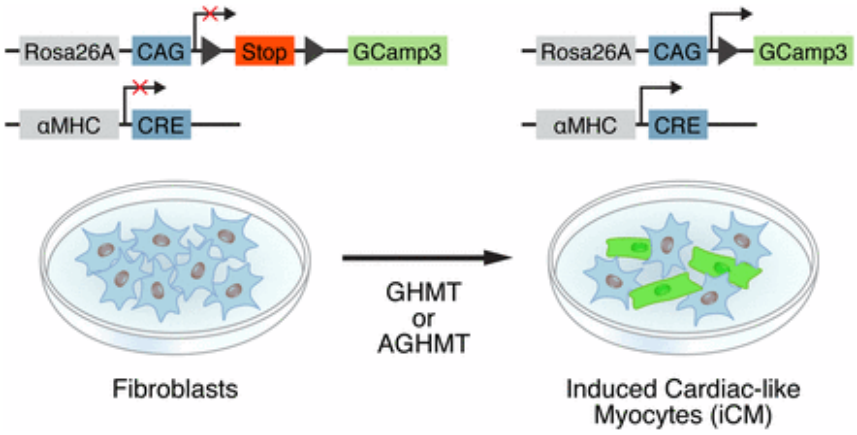

Figure 2-8 Strategy for measuring calcium flux.

MEFs derived from αMHC-Cre/Rosa26A-Flox-Stop-Flox-GCaMP3 transgenic mice were reprogrammed to iCMs by addition of GHMT or AGHMT and exhibit spontaneous cyclic autofluorescence concomitant with calcium flux.

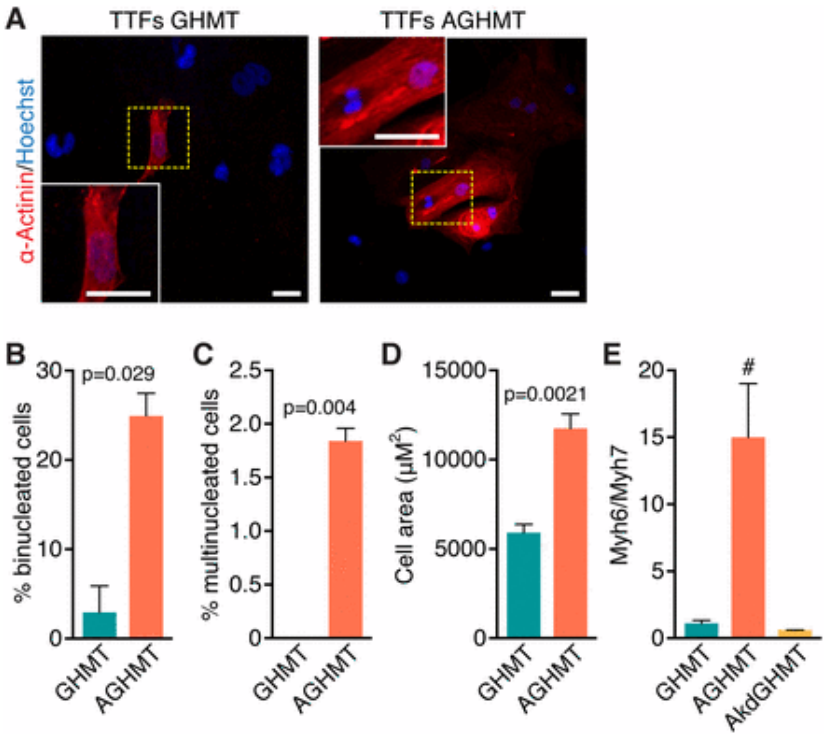

Figure 2-9 Addition of Akt1 to GHMT stimulates maturation of iCMs in TTFs.

(A) α-Actinin immunostaining shows binucleate iCM 3 wk after induction with GHMT and AGHMT. (Scale bars: 25 μm.) (B and C) Quantification of the percentage of iCMs with more than a single nucleus (binucleate, two nuclei; multinucleate, three or more nuclei) 3 wk after AGHMT treatment reveals an increase relative to cells treated with GHMT. (D) Size of iCMs was approximately doubled by addition of Akt1 to GHMT, as shown here 3 wk after induction after immunocytochemistry for α-actinin. (E) The ratio of Myh6:Myh7 by qPCR in TTFs 1 wk after induction suggests that adding Akt1 to GHMT results in more mature iCMs whereas a kinase dead mutant of Akt1 abrogates this effect. #$P < 0.05$ vs. all others.

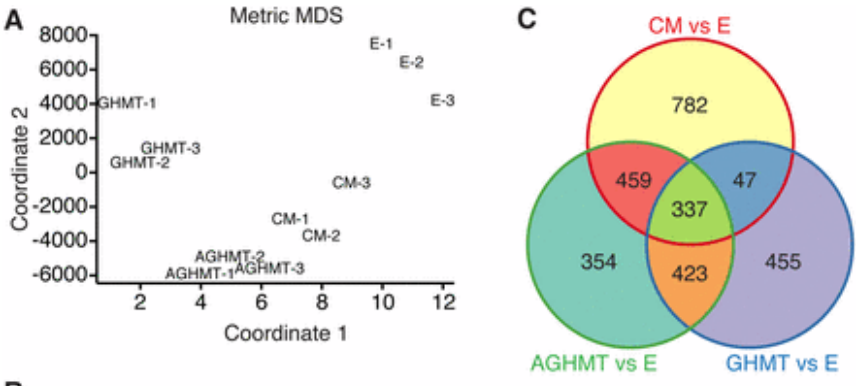

B

Comparison	Up	Down	Total
AGHMT vs GHMT	216	4	220
AGHMT vs CM	556	688	1244
AGHMT vs E	826	747	1573
GHMT vs CM	732	1601	2333
GHMT vs E	290	972	1262
CM vs E	986	639	1625

Figure 2-10 RNA-Seq global analysis shows that AGHMT iCMs are more similar to mature CM than GHMT iCMs.

(A) Multidimensional scaling (MDS) plot showing RNA-Seq sample relatedness based on 2D coordinates. Distance measurements were calculated using normalized RNA expression values from all expressed markers in each sample. (B) Count table for differentially expressed markers for various sample group comparisons using fold change cutoff of ≥2 and P value of ≤0.01. (C) Venn diagram showing number of overlapping markers between GHMT, AGHMT, and CM compared with empty vector control. Marker counts include both up-regulated and down-regulated genes.

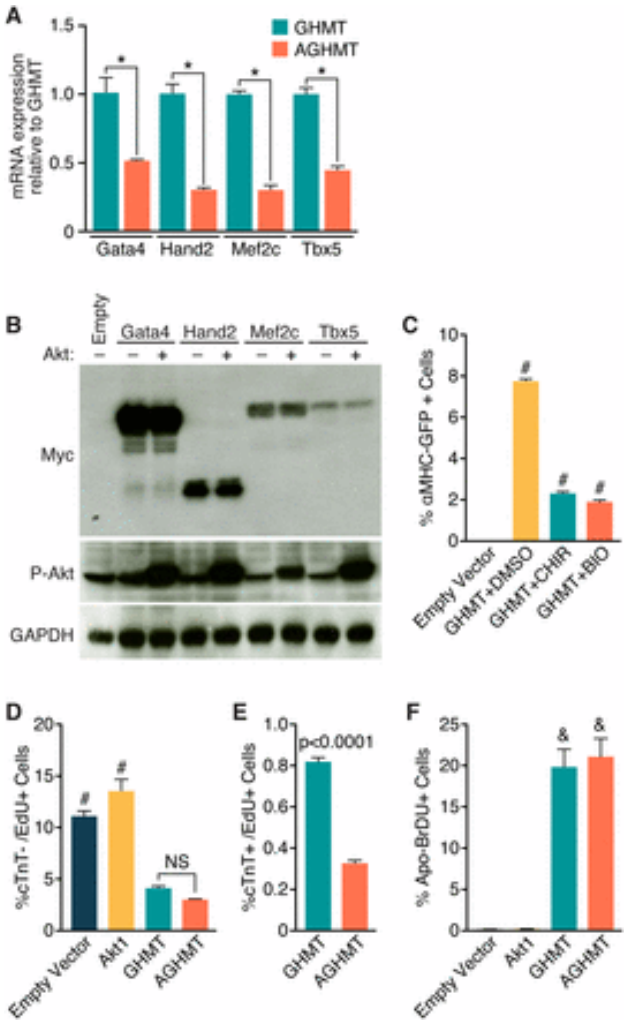

Figure 2-11 Processes not involved in the mechanism by which Akt1 enhances GHMT-mediated formation of iCMs.

(A) Measurement of Gata4, Hand2, Mef2c, or Tbx5 transcript by qPCR after 7 d of induction in GHMT- or AGHMT-treated MEFs. (B) Western blot of myc-tagged GHMT proteins in the presence or absence of Akt1 in MEFs after 2 d of induction. (C) Flow cytometry analysis after 7 d of GHMT treatment in MEFs (derived from aMHC-GFP mice) in the presence or absence of CHIR99021 (CHIR) or BIO. (D and E) Flow cytometry analysis of MEFs treated with Edu for 1 h following 7 d induction with control, Akt, GHMT, or AGHMT. Cardiac troponin T (cTnT) labels iCMs and Edu labels proliferating cells. (F) Flow cytometry analysis was used to measure apoptosis of MEFs following 7 d induction with control, Akt, GHMT, or AGHMT. Addition of Akt had no significant effect on apoptosis as measured by this assay. *P < 0.05; #P < 0.05 vs. all others; &P < 0.05 vs. all others unless also labeled with "&".

2.2 REFERENCES

1. Xin M, Olson EN, & Bassel-Duby R (2013) Mending broken hearts: cardiac development as a basis for adult heart regeneration and repair. Nat Rev Mol Cell Biol 14(8):529-541.

2. Ieda M, et al. (2010) Direct reprogramming of fibroblasts into functional cardiomyocytes by defined factors. Cell 142(3):375-386.

3. Inagawa K, et al. (2012) Induction of cardiomyocyte-like cells in infarct hearts by gene transfer of Gata4, Mef2c, and Tbx5. Circ Res 111(9):1147-1156.

4. Jayawardena TM, et al. (2014) MicroRNA Induced Cardiac Reprogramming In Vivo: Evidence for Mature Cardiac Myocytes and Improved Cardiac Function. Circ Res 116(3):418-424.

5. Nam YJ, et al. (2013) Reprogramming of human fibroblasts toward a cardiac fate. Proc Natl Acad Sci USA 110(14):5588-5593.

6. Qian L, et al. (2012) In vivo reprogramming of murine cardiac fibroblasts into induced cardiomyocytes. Nature 485(7400):593-598.

7. Song K, et al. (2012) Heart repair by reprogramming non-myocytes with cardiac transcription factors. Nature 485(7400):599-604.

8. Spater D, Hansson EM, Zangi L, & Chien KR (2014) How to make a cardiomyocyte. Development 141(23):4418-4431.

9. Sadahiro T, Yamanaka S, & Ieda M (2015) Direct Cardiac Reprogramming: Progress and Challenges in Basic Biology and Clinical Applications. Circ Res 116(8):1378-1391.

10. Yang X, Pabon L, & Murry CE (2014) Engineering adolescence: maturation of human pluripotent stem cell-derived cardiomyocytes. Circ Res 114(3):511-523.

11. Bock-Marquette I, et al. (2009) Thymosin beta4 mediated PKC activation is essential to initiate the embryonic coronary developmental program and epicardial progenitor cell activation in adult mice in vivo. J Mol Cell Cardiol 46(5):728-738.

12. Condorelli G, et al. (2002) Akt induces enhanced myocardial contractility and cell size in vivo in transgenic mice. Proc Natl Acad Sci USA 99(19):12333-12338.

13. Gude N, et al. (2006) Akt promotes increased cardiomyocyte cycling and expansion of the cardiac progenitor cell population. Circ Res 99(4):381-388.

14. Cahan P, et al. (2014) CellNet: network biology applied to stem cell engineering. Cell 158(4):903-915.

15. Nam YJ, et al. (2014) Induction of diverse cardiac cell types by reprogramming fibroblasts with cardiac transcription factors. Development 141(22):4267-4278.

16. Patel RK & Jain M (2012) NGS QC Toolkit: a toolkit for quality control of next generation sequencing data. PloS One 7(2):e30619.

17. Li H & Durbin R (2009) Fast and accurate short read alignment with Burrows-Wheeler transform. Bioinformatics 25(14):1754-1760.

18. Anders S & Huber W (2010) Differential expression analysis for sequence count data. Genome Biol 11(10):R106.

19. Anders S, et al. (2013) Count-based differential expression analysis of RNA sequencing data using R and Bioconductor. Nat Protoc 8(9):1765-1786.

20. Huang DW, et al. (2007) DAVID Bioinformatics Resources: expanded annotation database and novel algorithms to better extract biology from large gene lists. Nucleic Acids Res 35(Supplement 2):W169-W175.

21. Furtado MB, et al. (2014) Cardiogenic genes expressed in cardiac fibroblasts contribute to heart development and repair. Circ Res. 114(9):1422-34.

22. Zhou et al (2015) Akt1/protein kinase B enhances transcriptional reprogramming of fibroblasts to functional cardiomyocytes. PNAS. 112: 3811864–11869,

23. Zhou et al (2015) Akt1/protein kinase B enhances transcriptional reprogramming of fibroblasts to functional cardiomyocytes. PNAS. 112: 3811864–11869

CHAPTER 3. ACTIVATION OF CARDIAC ENHANCERS AND INHIBITION OF THE INFLAMMATORY RESPONSE PROMOTES CARDIAC REPROGRAMMING OF ADULT FIBROBLASTS

.

3.1 ACTIVATION OF CARDIAC ENHANCERS AND INHIBITION OF THE INFLAMMATORY RESPONSE PROMOTES CARDIAC REPROGRAMMING OF ADULT FIBROBLASTS

3.1.1 Abstract

Direct reprogramming of fibroblasts to cardiomyocytes represents a potential means of restoring cardiac function following myocardial injury. We previously reported that addition of Akt in the presence of four cardiogenic transcription factors, Gata4, Hand2, Mef2c, and Tbx5 (AGHMT), efficiently activates the cardiac gene program in ~50% of mouse embryonic fibroblasts. However, only ~1% of adult tail-tip fibroblasts acquire a contractile phenotype under these conditions, suggesting the existence of barriers to the reprogramming process. To identify additional regulators of adult cardiac reprogramming, we carried out an unbiased screen of 1,126 open reading frame cDNAs encoding transcription factors and cytokines for those that could enhance or suppress the cardiogenic activity of AGHMT. This screen led to the discovery of 50 new inducers and 133 repressors of cardiac reprogramming. One of the strongest activators of cardiac reprogramming was Krüppel-Type Zinc-Finger Transcription Factor 281 (ZNF281). Although ZNF281 lacks autonomous cardiogenic activity, we show that it enhances cardiac reprogramming by associating with GATA4 on cardiac enhancers and by inhibiting inflammatory signaling, which antagonizes cardiac reprogramming. These results identify

ZNF281 as a robust and efficient inducer of adult cardiac reprogramming and provide new insights into the molecular mechanisms underlying the cardiac phenotype.

3.1.2 Introduction

A heart attack (also known as myocardial infarction (MI)) occurs when the flow of blood to the heart is obstructed. Following a massive MI, the human heart can lose hundreds of millions of cardiomyocytes. Due to the limited capacity of the heart to regenerate, the lost cardiomyocytes are replaced by scar tissue, thus impairing contractility of a large portion of the heart muscle. Clinical interventions following a heart attack have improved dramatically over the past decades (1). However, due to the inability of the heart to replenish lost cardiomyocytes, MI remains the primary cause of death in the world(1, 2). Fifty percent of the heart is comprised of cardiac fibroblasts (CFs), which upon injury are activated and contribute to the formation of scar tissue(3). Reprogramming CFs in the heart to induced-cardiomyocytes (iCMs) by forced expression of cardiac specific transcription factors represents a potential means of enhancing cardiac repair by reducing scar tissue while simultaneously generating new cardiomyocytes(4-8). However, low efficiency as well as the lack of understanding of the molecular basis of the reprogramming process represent challenges to its potential clinical application(9-11).

Considerable effort has been directed toward optimization of cardiac reprogramming by generating different cocktails that contain various combinations of proteins, microRNAs, and small molecules(12-20). We previously reported that a cocktail containing Akt1, Gata4, Hand2, Mef2c, and Tbx5 (AGHMT, we refer to this as 5F hereafter) converts ~50% of mouse embryonic fibroblasts (MEFs) to iCMs(12). However, the efficiency of conversion of adult tail-tip fibroblasts (ATTFs) is less than 1%. Since heart attacks primarily occur in adults, and since the

human population is increasing in age, inefficient reprogramming of adult fibroblasts to iCMs diminishes the clinical translatability of this technique(12). Given that the efficiency of reprogramming embryonic fibroblasts is substantially higher than for adult fibroblasts, we reasoned that additional unidentified regulators are needed to reprogram adult fibroblast to iCMs.

Here we report performing an unbiased screen using 1,126 open reading frame cDNAs (ORFs) encoding 700 transcription factors, 280 cytokines, 85 epigenetic regulators and 61 nuclear receptors to augment 5F cardiac reprogramming of ATTFs. This screen led to the discovery of 50 inducers and 133 repressors of cardiac reprogramming. Many of these identified factors would not have been anticipated to impinge on the mechanisms of fibroblast-to-cardiomyocyte reprogramming. Among the 50 identified inducer factors, the strongest activator of cardiac reprogramming was Krüppel-Type Zinc-Finger Transcription Factor 281 (Znf281). We determined that Znf281 enhanced cardiac reprogramming by two mechanisms: 1) Gata4 recruits Znf281 to cardiac enhancers to directly promote cardiac gene expression and 2) Znf281 inhibits inflammatory signaling which potently antagonizes cardiac reprogramming. These results not only identify ZNF281 as a robust and efficient inducer of adult cardiac reprogramming, but also provide new insights into the molecular mechanisms underlying direct cardiac reprogramming.

3.1.3 Materials and Methods

3.1.3.1 Mice

All protocols involving animals in this paper were approved by the Institutional Animal Care and Use Committee at the University of Texas Southwestern Medical Center.

3.1.3.2 Cell culture and treatment

TTFs and CFs were prepared as described (refs). Retroviral transduction and cellular reprogramming were performed as described (refs). Reprogramming medium (Ref) contains DMEM/199 (4:1), 10% FBS, 5% horse serum, 1%penicillin and streptomycin, 1% non-essential amino acids, 1% essential amino acids, 1% B-27, 1% insulin-selenium-transferrin, 1% vitamin mixture, and 1% sodium pyruvate (Invitrogen). Small molecule treatments were used either throughout the reprogramming process [10 μM dexamethasone (Dex), 10 μM nabumetone (Nab), Sigma.X.

3.1.3.3 Construction of human retroviral ORFs library and production of retroviruses.

Gateway-compatible Human ORFs pEntry vectors were purchased from Thermo Fisher Scientific. Gateway-compatible retroviral destination vector, pMXs-GW, was obtained from Addgene (#18656). We transferred each ORF individually into pMXs-GW by performing site-specific LR recombination using Gateway LR Clonase II Enzyme Mix kit (Thermo Fisher Scientific).

3.1.3.4 Flow Cytometry

For Flow Cytometry, cells were trypsinized and fixed with fixation buffer (BD Bioscience) for 15 min on ice. Fixed cells were washed with Perm/Wash buffer (BD Bioscience) for three times. Washed cells were incubated with mouse monoclonal anti-cardiac Troponin T (cTnT) antibody (Thermo Scientific) at 1:200 dilution and Rabbit anti-GFP antibody (Thermo Scientific) at 1:200 dilution in Perm/Wash buffer for 1 h on ice. Cells then were washed with Perm/Wash buffer for three times followed by incubation with donkey anti-mouse Alexa fluor 647 (Invitrogen) at 1:200 and Goat anti-Rabbit Alexa fluor 488 at 1:200 (Invitrogen). Cells were

washed with Perm/Wash buffer, and then analyzed using FACS Caliber (BD Sciences) and FlowJo software.

3.1.3.5 Immunocytochemistry

For immunocytochemistry, cells were fixed in 4% paraformaldehyde for 15 min and permeabilized with 0.1% Triton-X in room temperature. Cells were washed with PBS for three times followed by blocking with 10% Goat serum for 1h. Cells then were incubated with mouse monoclonal anti-cardiac Troponin T (cTnT) antibody (Thermo Scientific) at 1:500 dilutions and Rabbit anti-GFP antibody (Thermo Scientific) at 1:500 dilutions in 5% Goat serum for 1 h. After washing with PBS three times, Cells then were incubated with donkey anti-mouse Alexa fluor 647 (Invitrogen) at 1:500 and Goat anti-Rabbit Alexa fluor 488 at 1:500 (Invitrogen).

3.1.3.6 Quantitative mRNA measurement, Co-IP and western blot analyses

Total RNA was extracted using TRIzol (Invitrogen) according vender's protocol. RNAs were retrotranscribed to cDNA using iScript Supermix (Bio-Rad). qPCR was performed using Kapa Sybr Fast (Kapa Biosystems). Co-IP and western blot analyses were performed as described (13), using Flag antibody (1:1,000,), Myc antibody antibody (1:1,000).

3.1.3.7 Differential Gene Expression Analysis

We performed RNA-Seq using the Next Generation Sequencing Core at the University of Texas Southwestern Medical Center. Three micrograms of DNAse-treated RNA per replicate were prepared using the TruSeq Stranded LT Kit from Illumina. Samples were then PCR amplified and purified with Ampure XP beads before sequencing on a HiSeq2500 instrument (Illumina, Inc., San Diego, CA). All procedures were carried out according to manufacturer

protocols. Quality assessment of the RNA-Seq data was done using NGS-QC-Toolkit. Reads with mean phred quality scores of less than 20 were removed from further analysis. Quality filtered reads were then aligned to the mouse reference genome GRCm38 (mm10) using the Bowtie2 (v 2.0.6) aligner. Only uniquely mapped reads were kept for further downstream analysis. Differential gene expression analysis was done using the R package DESeq (v 1.10.1) following the protocols outlined in. Read counts were normalized by taking the median of each gene count across samples and dividing each sample gene count by the relative ratio of library sizes between the calculated median and sample size. The averaged normalized expressions values of the triplicate samples were used to calculate fold change and p-values. Cutoff values of fold change greater than two and p- value less than 0.01 were then used to select for differentially expressed genes between sample group comparisons.

3.1.3.8 Pathway Enrichment Analysis

Significant pathway enrichment analysis was performed using Ingenuity Pathways Analysis (Ingenuity® Systems, Redwood City, CA). Differentially expressed genes from the RNA expression data are associated with a biological function supported by at least one publication in the Ingenuity® Pathways Knowledge Base. Fisher's exact test is then used to calculate the p-value and determine the probability that each biological function is enriched in the dataset due to chance alone. Statistically significant biological pathways were then identified by selection for pathways with p-values less than 0.05. DAVID gene functional annotation and classification tool was used to annotate the list of differentially expressed genes with respective Gene Ontology terms and perform GO enrichment analysis for molecular and biological

functional categories. Functional Gene Ontology groups were selected for significance by using a p-value cutoff of 1%.

3.1.3.9 Statistical Analyses

All in vitro data are presented as mean with S.E.M. and have N=3 per group. P- values were calculated with either unpaired/two-way t-test or one-way ANOVA, as appropriate, except in time-course analyses where we utilized two-way ANOVA. All statistical analyses were run using the GraphPad Prism 6 software package (GraphPad Software, Inc., La Jolla, CA). $P<0.05$ was considered significant in all cases after corrections were made for multiple pairwise comparisons.

3.1.4 Results

3.1.4.1 Identification of inducers and inhibitors of cardiac reprogramming in adult fibroblasts

We previously established a cardiac reprogramming protocol by expressing Akt kinase and a cocktail of cardiac transcription factors (Gata4, Hand2, Mef2c and Tbx5, (referred to as 5F hereafter), in tail tip fibroblasts (TTFs) isolated from a transgenic mouse containing an α-myosin heavy chain (αMHC)-GFP transgene, which is expressed specifically in cardiomyocytes (8). Using this 5F reprogramming protocol, we achieved ~3% efficiency of reprogramming of TTFs to iCMs as measured by αMHC-GFP and immunostaining with cardiac troponin T (cTnT) (12). To identify additional regulators of cardiac reprogramming, we created a retroviral expression library consisting of ~1,100 human cDNAs encoding 700 transcription factors, 280 cytokines, 85 epigenetic regulators and 61 nuclear receptors. We screened this expression library for activators

and suppressors of cardiac reprogramming by expressing individual cDNAs together with 5F in isolated TTFs from αMHC-GFP mice. After 9 days, 5F reprogrammed TTFs were assessed by αMHC-GFP and cTnT expression (Figure 3-1A). A high-throughput cell analyzer system was used to image and quantify cardiac reprogramming based on αMHC-GFP and cTnT expression. (Figure 1B). Inducers were defined as genes activating αMHC-GFP or cTnT expression by ≥2-fold, whereas genes with scores ≤-2 for αMHC-GFP or cTnT expression were defined as repressors. This screen led to the discovery of 50 potential inducers and 133 potential repressors of cardiac reprogramming (Figure 3-1C and D).

Among the 50 inducers, 25 enhanced αMHC-GFP expression; 36 enhanced cTnT expression; and 11 enhanced expression of both cardiac markers (Figure 3-1C). The two strongest inducers were PHD finger protein 7 (PHF7), a histone H3 binding protein expressed only in the male germ line (21); and Zinc finger protein 281 (ZNF281), a zinc finger transcription factor about which little is known (Figure 1B, Table S2). Among the 133 repressors, 123 inhibited αMHC-GFP expression; 43 inhibited cTnT expression; and 33 inhibited both cardiac markers (Figure 1C). Some of the repressors, such as forkhead box protein A3 (FOXA3), practically abolished 5F-mediated cardiac reprogramming (Figure 3-1B).

To identify key pathways that regulate cardiac reprogramming, we performed pathway enrichment analysis for inducer and suppressor genes. Intriguingly, the most enriched pathways associated with inducers fell into the inflammatory stress response category, such as regulation of interferon-A (IFNA) signaling and cytokine signaling in the immune system (Figure 3-1E). The top enriched pathways associated with repressors fell into the nuclear receptor transcriptional pathway and developmentally regulated pathway categories, such as

regulation of β-cell development and activation of HOX genes during differentiation. Two pathways, interleukin-4 and -13 signaling and the senescence-associated secretory phenotype, which are associated with inflammatory and stress responses, were also enriched among the functions associated with the suppressors (Figure 3-1F).

Since inflammatory and stress response signaling pathways were found to be associated with both inducers and suppressors, we examined the functions of each of the individual inducers and repressors within those pathways. Interestingly, we found that most inducers possessed anti-inflammatory functions, including several anti-inflammatory cytokines, such as IFNA2, IFNA16 and IL10; whereas most repressors have pro-inflammatory functions, including several pro-inflammatory cytokines, such as IL1A, IL11 and IL26 (Figure 3-1G). Given that inducers and repressors were associated with opposing inflammatory functions, we postulated that inflammatory mechanisms likely impose a barrier to cardiac reprogramming, whereas inhibition of inflammatory responses by anti-inflammatory factors might enhance reprogramming.

3.1.4.2 Anti-inflammatory drugs promote direct cardiac reprogramming

Our findings suggested that the inflammatory response is likely a barrier for cardiac reprogramming (Figure 3-1E-G). We suspected that inhibition of the inflammatory response by anti-inflammatory drugs would also enhance reprogramming, so we tested two anti-inflammatory drugs, dexamethasone (Dex), a steroidal anti-inflammatory drug, and the PTGS1/2 inhibitor nabumetone (Nab), a non-steroidal anti-inflammatory drug on the reprogramming process. Anti-inflammatory drugs (10uM) were added on 5F-mediated reprogrammed TTFs post-viral infection. After 7 days of drug treatment, we harvested RNA and examined the transcript levels of inflammatory markers (IL6, Ccl2, and Ptgs1) and cardiac marker genes

(Myh6, Actc1 and Nppa) and by q-PCR. Addition of anti-inflammatory drugs to 5F decreased inflammatory marker expression as expected, but increased the expression of cardiac markers 2- to 10-fold, indicating enhanced reprogramming efficiency (Figure 3-2A).

To further confirm the cardiogenic capacity of anti-inflammatory drugs in cardiac reprogramming, we performed immunocytochemistry (Figure 2B) and flow cytometry (Figure 3-2C) for the cardiac markers αMHC-GFP and cTnT. Both results confirmed the capacity of anti-inflammatory drugs to promote cardiac reprogramming (Figure 3-2B and C).

3.1.4.3 ZNF281 enhances cardiac reprogramming in adult fibroblasts

PHF7 and ZNF281 were the two strongest inducers identified from our retroviral cDNA expression screen with 5F (Figure 1B and Table S2). PHF7 is only expressed in the male germ line (21), whereas ZNF281 has a broad expression pattern with enriched expression in the heart (Figure S1). We therefore focused our initial attention on ZNF281 and explored its ability to enhance the activity of 5F. We refer to our reprogramming mix of 5F plus ZNF281 as 6F hereafter. We validated the results of our screen by assessing GFP and cTnT expression in αMHC-GFP TTFs following 5F and 6F reprogramming after 7 days (Figure 3-3A).

Flow cytometry analysis showed that addition of ZNF281 to 5F generated ~33% of αMHC-GFP+, ~45% cTnT+ and ~28% of αMHC-GFP+/ cTnT+ TTFs after 7 days of reprogramming (Figure 3-3B). This TTF reprogramming efficiency using 6F is noteworthy when considering that the relatively low statistical likelihood of each fibroblast taking up all five or six separate retroviruses encoding the reprogramming factors. We also examined the transcript level of cardiac and fibroblast marker genes by q-PCR. Addition of ZNF281 to 5F increased the

expression of cardiac marker genes, Myh6 and Actc1, to ~120-fold and ~20-fold, respectively, and decreased fibroblast marker genes, Col1a2 and Sox9, to ~30% and ~60%, respectively (Figure 3-3C).

We performed RNA-seq using TTFs reprogrammed for 7 days with 5F or 6F. Using a two-fold cutoff and FDR < 0.01 threshold for inclusion, we identified ~1,000 up-regulated genes and 500 down-regulated genes in 6F compared to 5F (Figure 3-4A-E). We performed gene ontology enrichment analysis in the up- and down-regulated genes separately. As anticipated, most gene ontology terms enriched in the up-regulated genes were cardiac related (Figure 3-4B and D), suggesting that ZNF281 globally enhanced cardiac reprogramming. Interestingly, the top gene ontology terms enriched in the down-regulated genes were all related to the inflammatory response (Figure 3-3C and E), suggesting a dual role for ZNF281 in activation of cardiac and suppression of inflammatory gene programs.

3.1.4.4 ZNF281 is a cardiac coactivator of GATA4

To Little is known of the functions of ZNF281. To begin to define the molecular mechanism whereby ZNF281 enhances cardiac reprogramming, we performed co-immunoprecipitation assays for ZNF281 with each reprogramming transcription factor in transfected HEK293 cells. We found that FLAG-tagged ZNF281 indeed co-immunoprecipitated with Myc-tagged GATA4 but not with the other three factors (Figure 3-5A).

To determine if ZNF281 could activate cardiac genes, we examined the ability of ZNF281 to activate a luciferase reporter controlled by the cardiac specific αMHC promoter (αMHC-Luciferase). We discovered that ZNF281 activated the αMHC-Luciferase reporter ~7-

fold (Figure 3-5B). When ZNF281 was co-expressed with GATA4, αMHC-Luciferase was activated ~15-fold (Figure 3-5B), suggesting that ZNF281 and GATA4 synergize to activate the αMHC promoter. The finding that ZNF281 alone activates the αMHC promoter within the reporter, but could not activate this or other endogenous cardiac genes alone may suggest that it relies on GATA4 as a pioneer factor to open target sites on cardiac genes that are otherwise inaccessible in native chromatin.

3.1.4.5 ZNF281 broadly co-occupied cardiac enhancers with GATA4

To understand the molecular relationship between ZNF281 and GATA4 in the cardiac reprogramming process, we examined the genomic locations of ZNF281 and GATA4 at an early stage of the reprogramming process (2 days post-infection of 6F) by chromatin immunoprecipitation (ChIP) (Figure 3-5C). We performed de novo motif discovery on the binding peaks for ZNF281 and GATA4. The most significantly enriched motif associated with ZNF281 binding was GGGGTGGGG (Figure 3-5D). For GATA4, the most enriched motif was GATAAG, which matches the consensus sequence for DNA binding of this transcription factor (Figure 3-5E). Chip-seq sequencing identified 14,623 peaks for ZNF281 and 30,664 peaks for GATA4 (Figure 3-5F). Based on the interaction of ZNF281 with GATA4 (Figure 3-5A), we predicted that ZNF281 co-occupies genomic sites with GATA4. Indeed, among the 14,623 peaks of ZNF281, we found 13,392 of them (91.6%, 13,392/14623) overlapping with peaks of GATA4, indicating extensive co-binding of ZNF281 and GATA4 to endogenous genomic sites at an early stage of the cardiac reprogramming process (Figure 3-5F). To assess genome-wide localization of ZNF281 on cardiac enhances, we established a cardiac enhancers landscape using Encode H3K27ac ChIP-seq. We found that 7,357 peaks associated with ZNF281 were on cardiac

enhancers, which accounted for 50.4% of total peaks of ZNF281, indicating ZNF281 broadly binds on cardiac enhancers (Figure 3-5F).

3.1.4.6 GATA4 recruits ZNF281 to cardiac enhancers

We compared the occupancy patterns of ZNF281 and GATA4 in the presence (6F) or absence of GATA4 (6F-G). Additionally, we examined the occupancy pattern in the absence of ZNF281 (6F-Z) following reprogramming. We found that the occupancy pattern of GATA4 on the genome was not dramatically affected by the presence or absence of ZNF281 (Figure 6A, lower panel). However, the presence or absence of GATA4 strongly impacted the genomic occupancy pattern of ZNF281 (Figure 6A, upper panel). We assigned ZNF281 binding peaks into three clusters based on how GATA4 influenced ZNF281 occupancy: a GATA4-dependent cluster (cluster1, 8882/33934); a GATA4-independent cluster (cluster2, 7003/33934); and a GATA4-inhibited cluster (cluster3, 18049/33934) (Figure 3-6A and B). Interestingly cluster3, in which the occupancy of ZNF281 was inhibited by the presence of GATA4, also correlated with lower binding affinity of GATA4 compared with clusters 1 and 2 (Figure 3-5A). It seems that the higher-affinity GATA4 binding sites in cluster 1 competed ZNF281 away from the lower affinity GATA4 binding sites in cluster 3.

To investigate the functional significance of the GATA4 and ZNF281 binding peaks in the three clusters, we performed gene ontology and pathway enrichment analysis using the Genomic Regions Enrichment of Annotations Tool (GREAT, (22)). For gene ontology enrichment analysis, we found that most gene ontology terms enriched in cluster 1 and 2 were heart or muscle related (Figure 6F), whereas most of the gene ontology terms enriched in cluster 3 were related to stress and inflammatory responses. For pathway enrichment analysis, several

pathways, such as the TGF-beta and Wnt signaling pathways, which are known to be important for cardiogenesis, heart repair and cardiac reprogramming (17), are enriched in clusters 1 and 2, whereas inflammatory response pathways are enriched in cluster 3 (Figure 3-6A). We conclude that GATA4 recruits ZNF281 to cardiac enhancers to activate cardiac gene expression.

3.1.4.7 ZNF281 represses the inflammatory response through the nucleosome remodeling deacetylase (NuRD) complex.

Our In contrast to the effect on cardiac enhancers, GATA4 did not have an impact on ZNF281 binding to inflammatory enhancers (Figure 6A and D). Additionally, ZNF281 served as a repressor instead of an activator for inflammatory genes, suggesting distinct mechanisms for ZNF281 to regulate cardiac gene activation and inflammation. Previously it was reported that ZNF281 recruits the Nucleosome Remodeling Deacetylase (NuRD) complex to the Nanog locus to regulate its expression in mouse embryonic stem cells (26, 27). The NuRD complex is an ATP-dependent chromatin remodeling complex that contains multiple subunits, including methyl CpG binding domain 3 (MBD3), metastasis associated 1 (MTA1), MTA2, MTA3, retinoblastoma binding protein 4 (RBBP4), RBBP7, GATAD2A and GATAD2B and histone deacetylases 1(HDAC1) and HDAC2. NuRD complex has been shown to repress inflammatory signaling (28).

We suspected that ZNF281 represses inflammatory signaling through the NuRD complex to enhance cardiac reprogramming, so we tested several NuRD complex subunits in cardiac reprogramming process. We overexpressed NuRD complex subunits MTA1, MTA2, MTA3, MBD3, GATAD2A, GATAD2B, RBBP4, HDAC1and HDAC2 on top of 5F in TTFs. After 7 days of reprogramming, we harvested RNA and examined the transcript levels of inflammatory

markers (IL6, Ccl2) and cardiac marker genes (Myh6, Actc1) by q-PCR. Addition of four of NuRD complex subunits (MTA1, MTA2, MTA3 and MBD1) to 5F decreased inflammatory marker expression, but increased the expression of cardiac markers, indicating enhanced reprogramming efficiency (Figure 7A). To further confirm the cardiogenic capacity of NuRD complex subunits in cardiac reprogramming, we performed flow cytometry (Figure 3-7B and C) for the cardiac markers αMHC-GFP and cTnT. The result confirmed the capacity of NuRD complex subunits to promote cardiac reprogramming (Figure 3-7B and C)). We conclude that ZNF281 represses inflammatory response through NuRD complex to activate cardiac reprogramming.

3.1.5 Discussion

Here we performed an unbiased screen for regulators of adult cardiac reprogramming and identified a total of 183 new inducers or repressors that belong to various biological pathways. Specifically, we found that anti- and pro-inflammatory factors evoke opposing effects on cardiac reprogramming. Whereas pro-inflammatory molecules prevent reprogramming, anti-inflammatory drugs profoundly enhance cardiac reprogramming. Among the identified inducers, the zinc finger transcription factor ZNF281 showed the most potent reprogramming activity. We demonstrated that the effect of ZNF281 on cardiac reprogramming was likely mediated by association with Gata4 on cardiac enhancers and by inhibition of inflammatory signaling, which antagonizes cardiac reprogramming, through the NurD complex. (Figure 3-7).

The retroviral library we made in this study, to best of our knowledge, is the most comprehensive retroviral library for transcription factors, cytokines, epigenetic regulators and nuclear receptors. Given the genome-wide nature, this library can be used to screen regulators for

reprogramming fibroblasts to other cell types, such as neurons or iPSC reprogramming; or can be used in any biological study that needs to genome-widely investigate genes in those categories. This study validates the retroviral cDNA expression library and provides proof-of-concept of its usefulness. In addition, the high-throughput imaging screen platform that we designed for this study can be leveraged for development of high-throughput small molecules or shRNAs screens to further enhance and accelerate cardiac reprogramming.

Our results show that the inflammatory response acts as a barrier for cardiac reprogramming. Treatment of 5F reprogrammed adult TTFs with anti-inflammatory drugs, dexamethasone and nabumetone, greatly enhanced cardiac reprogramming efficiency in vitro. Multiple stimuli can trigger the inflammatory response in cardiac reprogramming. Viral infection used for delivery of the reprogramming factors is one source of the inflammatory response. GATA4, one of the reprogramming factors, has also been shown to induce inflammation in fibroblasts (23). Furthermore, in the clinical setting, inflammation and inflammatory cell filtration are hallmarks of MI and reperfusion injury (24). Ischemic cardiac injury triggers inflammatory reactions accompanied by cytokine release and inflammatory cell filtration into the infarct region. Given that there are additional inducers of the inflammatory response in vivo, we suspect that anti-inflammatory drugs are likely to have a more profound effect for in vivo cardiac reprogramming. Dexamethasone and nabumetone are two common anti-inflammatory drugs that have been used clinically for decades. Our findings highlight the potential clinical application of these two drugs in cardiac reprogramming. Unlike cardiac reprogramming, it has been reported that the inflammatory response is necessary for iPSC reprogramming (25). The opposing effects

of inflammation on cardiac versus iPSC reprogramming efficiency suggest that these two types of reprogramming employ distinct regulatory mechanisms.

Addition of ZNF281 to 5F boosted reprogramming efficiency of adult TTFs from 3% to 30%. ZNF281 functions as a positive regulator of cardiogenesis by associating with GATA4 on cardiac enhancers; and as a negative regulator of inflammatory signaling, through recruiting the NurD complex. A previous report on ZNF281 focused on its pluripotency effect on stemness and epithelial-mesenchymal transition (EMT), however little is known about its role in cardiogenesis and inflammation. Using our 6F cardiac reprogramming assay, we show that ZNF281 interacts with the cardiac transcription factor GATA4 to synergistically activate cardiac genes. We speculate that ZNF281 may also have important functions in the heart. ZNF281 by itself did not bind to cardiac enhancers in fibroblasts but required the presence of GATA4 and other reprogramming factors, indicating that ZNF281 is unlikely to be a pioneer factor that opens chromatin. Direct reprogramming of fibroblasts to cardiomyocytes represents a distinct path to achieve the cardiac phenotype compared to embryonic stem cells or induced pluripotent stem cell derived cardiomyocytes. The discovery of the cardiogenesis function of ZNF281 suggests that in addition to its clinical benefit, cardiac reprogramming may serve as a platform to decipher the cardiac phenotype.

3.1.6 Figures

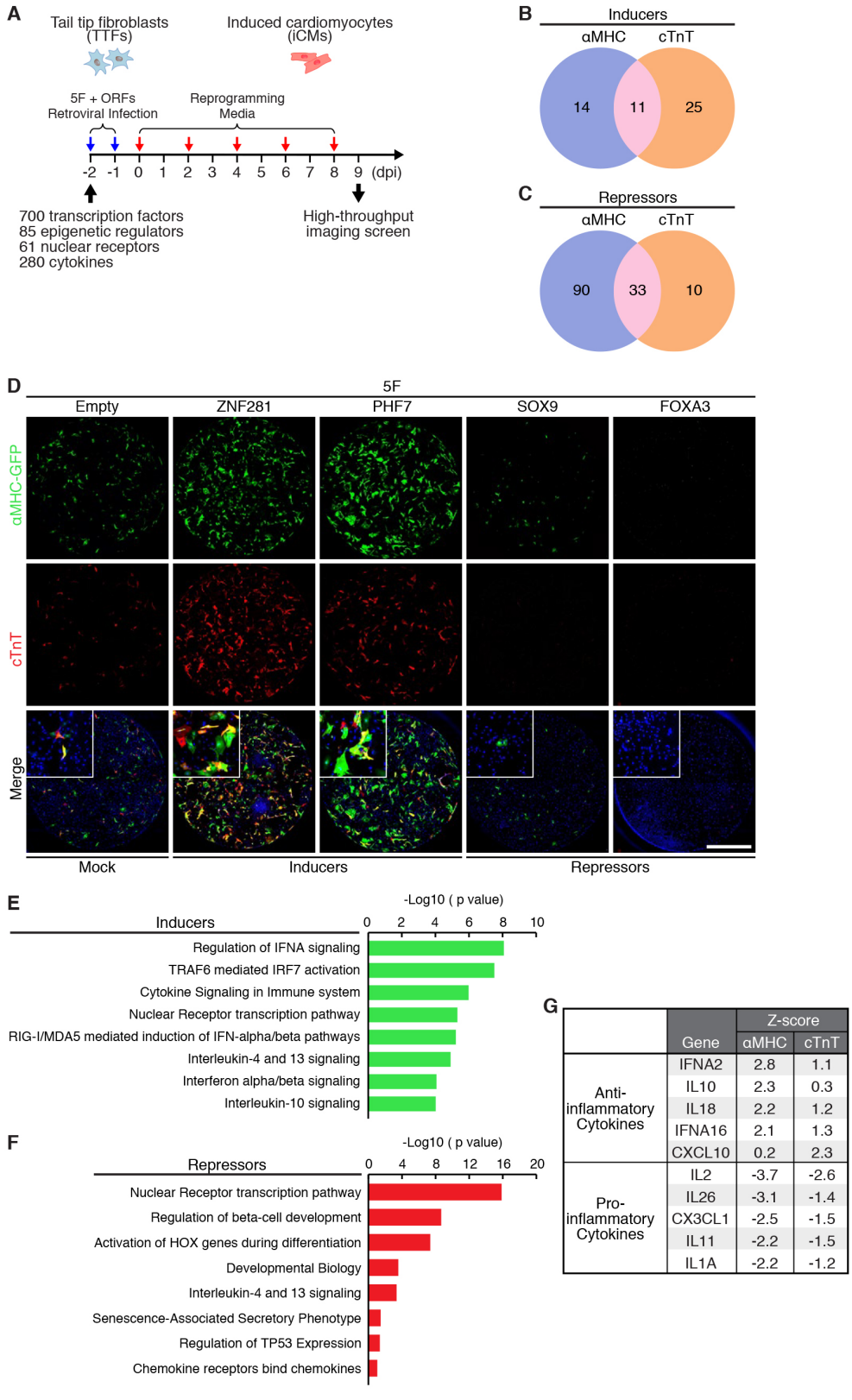

G

	Gene	Z-score αMHC	Z-score cTnT
Anti-inflammatory Cytokines	IFNA2	2.8	1.1
	IL10	2.3	0.3
	IL18	2.2	1.2
	IFNA16	2.1	1.3
	CXCL10	0.2	2.3
Pro-inflammatory Cytokines	IL2	-3.7	-2.6
	IL26	-3.1	-1.4
	CX3CL1	-2.5	-1.5
	IL11	-2.2	-1.5
	IL1A	-2.2	-1.2

Figure 3-1 Human ORF library screen identified inducers and inhibitors of cardiac reprogramming by AGHMT.

(A) Schematic diagram of the human ORF library screen for cardiac reprogramming in adult tail-tip fibroblasts (TTFs). (B) Representative immunocytochemistry screen images of control, two inducers (ZNF281 and PHF7) and two repressors (FOXA3 and SOX9) using TTFs isolated from adult αMHC-GFP transgenic mice. Cells were fixed and stained for αMHC-GFP(green), cTnT(red), DAPI(blue) 9 days post infection. 5F: AGHMT. (Scale bars: 2mm.). (C) Venn diagram showing number of inducers from the screen. Gene with Z-score of αMHC-GFP or cTnT expression ≥2 was defined as inducer. 25 genes induce αMHC expression, 36 genes induce cTnT expression and 11 genes induce both αMHC and cTnT expression. (D) Pathways enriched in inducers (n=50) by Reactome Pathway Analysis. (E) Venn diagram showing number of repressors from the screen. Gene with Z-score αMHC or cTnT expression ≤-2 was defined as repressors. 123 genes repress αMHC expression, 43 genes repress cTnT expression and 33 genes induce both αMHC and cTnT expression. (F) Pathways enriched in repressors (n=133) by Reactome Pathway Analysis. (G) Anti-inflammatory cytokines and pro-inflammatory cytokines were identified as inducers and repressors respectively.

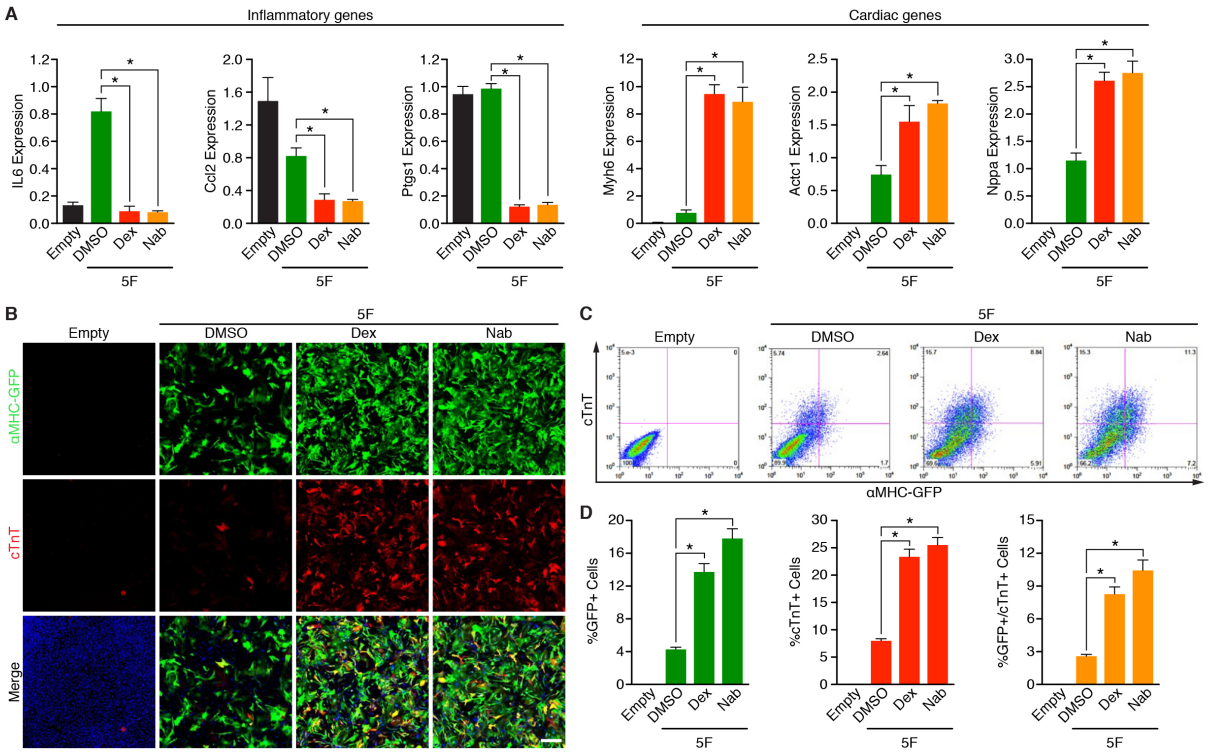

Figure 3-2 Anti-inflammatory drugs promote direct cardiac reprogramming.

(A) 5F reprogrammed TTFs treated with either DMSO or indicated anti-inflammatory drugs for 7 days of post infection, showing repressed expression of inflammatory genes (IL6, Ccl2, and Ptgs1), but increased expression of cardiac genes (Myh6, Actc1 and Nppa). Dex, Dexamethasone (10uM); Nab, Nabumetone (10uM). (B) Immunocytochemistry images of 5F reprogrammed adult αMHC-GFP transgenic TTFs treated with DMSO or indicated anti-inflammatory drugs for 7 days, showing Anti-inflammatory drugs enhances cardiac markers expression on top of 5F. αMHC-GFP (green), cTnT(red), DAPI(blue). (Scale bars: 500 μm). (C) Representative flow cytometry plot (top) and analyses (bottom) of αMHC-GFP+ and cTnT+ cells in 5F reprogrammed adult αMHC-GFP transgenic TTFs treated with DMSO or indicated anti-inflammatory drugs for 7 days, showing anti-inflammatory drugs increase the percentage of reprogrammed cells on top of 5F. *P<0.05

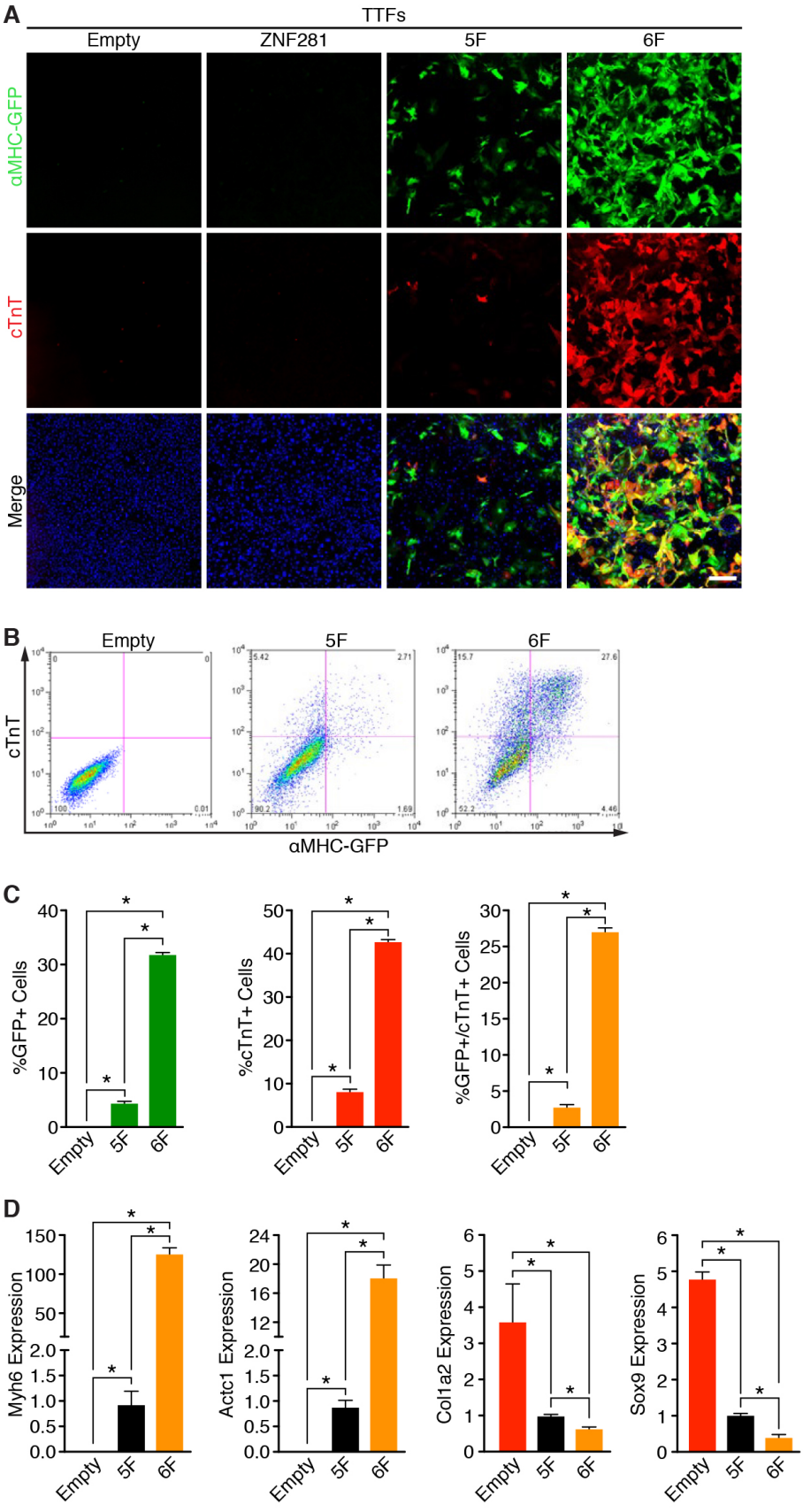
A
TTFs
Empty
ZNF281
5F
6F
αMHC-GFP
cTnT
Merge
B
Empty
5F
6F
cTnT
αMHC-GFP
C
%GFP+ Cells
%cTnT+ Cells
%GFP+/cTnT+ Cells
Empty
5F
6F
D
Myh6 Expression
Actc1 Expression
Col1a2 Expression
Sox9 Expression
Empty
5F
6F

Figure 3-3 ZNF281 enhances direct cardiac reprogramming in adults fibroblasts.

(A) Immunocytochemistry images of adult αMHC-GFP transgenic TTFs after 7 days infection with Empty, ZNF281, 5F, or 6F (5F+ZNF281) retrovirus, showing ZNF281 enhances cardiac markers expression on top of 5F. αMHC-GFP (green), cTnT(red), DAPI(blue). (Scale bars: 500 μm). (B) Representative flow cytometry plot (top) and analyses (bottom) of αMHC-GFP+ and cTnT+ cells in TTFs after 7days infection with Empty, 5F, or 6F retrovirus, showing ZNF281 increases the percentage of reprogrammed cells on top of 5F. (D) Transcript levels of cardiac marker genes (Myh6 and Actc1) and fibroblast marker genes were increased or decreased respectively a week after induction by adding ZNF281 to 5F in TTFs. * $P<0.05$.

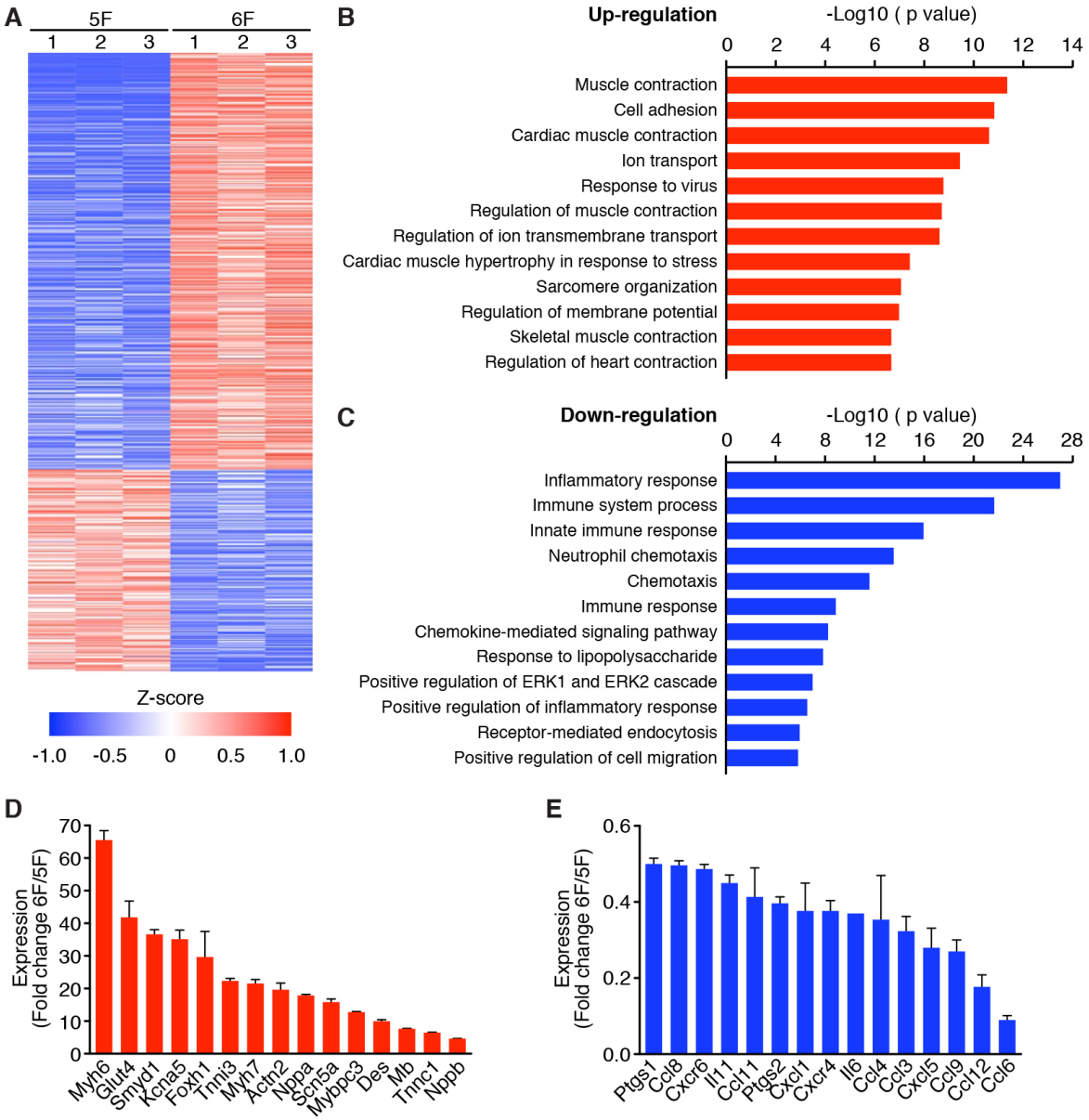

Figure 3-4 RNA-Seq analysis shows that ZNF281 enhances cardiac gene expression and repress inflammatory response.

(A) Heat map of 1,500 differentially expressed genes in 5F and 6F identified by RNA-seq. Red indicates up regulation, and blue indicates down regulation. RNA-seq samples were prepared from 7 days reprogrammed TTFs. (B and C) Gene ontology enriched in up regulated genes (B) and down regulated genes (C) identified by gene ontology enrichment analysis. (D and E) Gene expression change between 6F and 5F for selected cardiac markers (D) or inflammatory markers (E) as determined by RNA-seq.

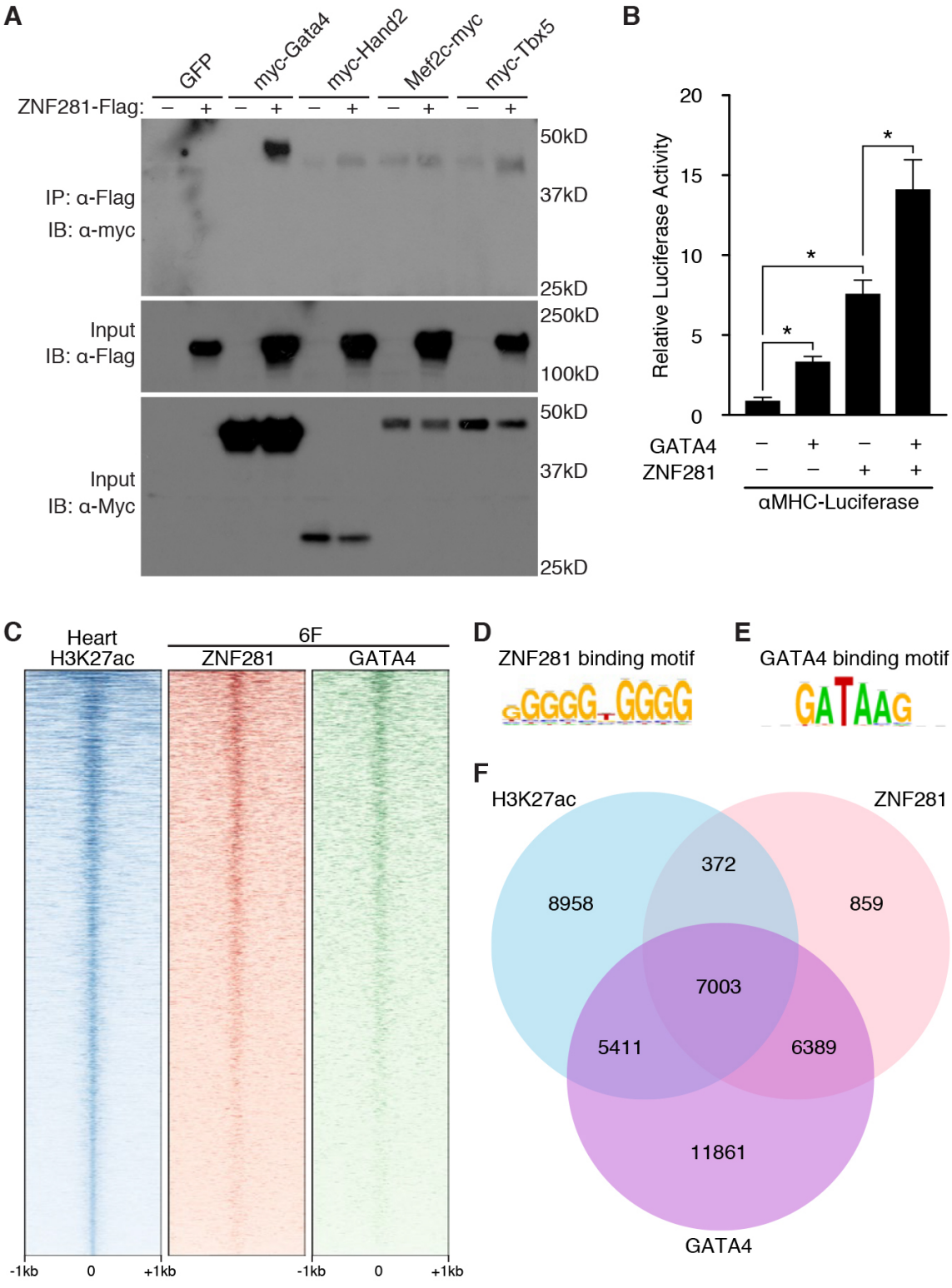
A
GFP
myc-Gata4
myc-Hand2
Mef2c-myc
myc-Tbx5
ZNF281-Flag: – + – + – + – + – +
IP: α-Flag
IB: α-myc
50kD
37kD
25kD
Input
IB: α-Flag
250kD
100kD
Input
IB: α-Myc
50kD
37kD
25kD
B
Relative Luciferase Activity
20
15
10
5
0
*
*
*
GATA4 – + – +
ZNF281 – – + +
αMHC-Luciferase
C
Heart
H3K27ac
6F
ZNF281
GATA4
-1kb
0
+1kb
-1kb
0
+1kb
D
ZNF281 binding motif
E
GATA4 binding motif
F
H3K27ac
ZNF281
GATA4
8958
372
859
7003
5411
6389
11861

Figure 3-5 ZNF281 interacts with GATA4 to synergistically activate cardiac promoter.

(A) Co-immunoprecipitation assays were performed using HEK293 cells transfected with equal amounts of Myc tagged Gata4, Hand2, Mef2c, or Tbx5 plasmid DNA and/or Flag tagged ZNF281. IP, immunoprecipitation; IB, immunoblot. (B) Luciferase reporter assay were performed using HEK293 cells transfected with equal amounts of ZNF281 and/or Gata4 expression plasmids, as indicated, along with αMHC-luciferase reporter plasmid. (C) Heat map for Heart H3K27ac, ZNF281 and GATA4 at ±5 kb around the peak center. ChIP-seq experiments were performed using 2 days reprogrammed TTFs infected with 6F. (D) Venn diagram showing number of overlapping peaks between Heart H3K27ac, ZNF281 and GATA4. *$P<0.05$

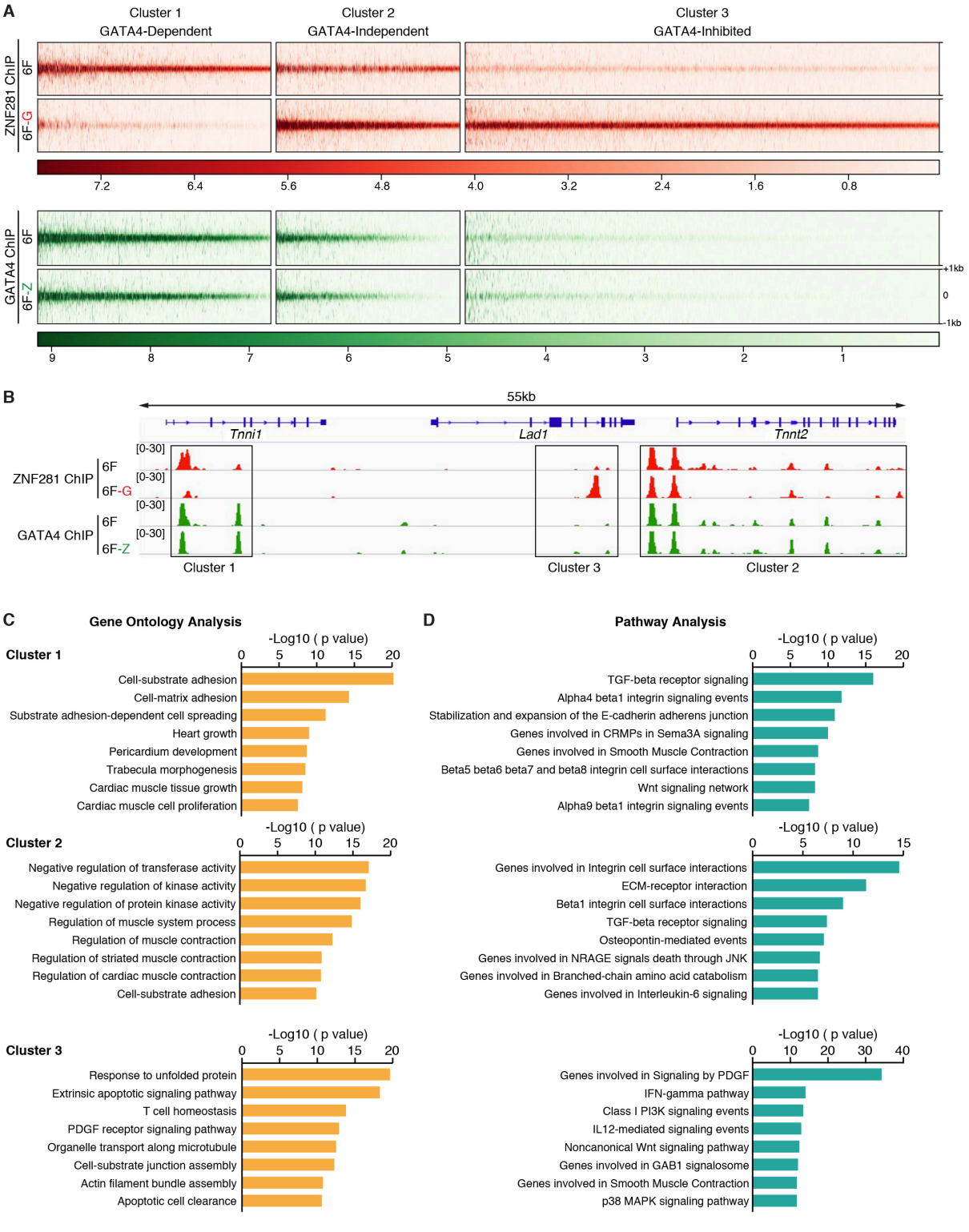
A
Cluster 1
GATA4-Dependent
Cluster 2
GATA4-Independent
Cluster 3
GATA4-Inhibited
ZNF281 ChIP
6F
6F-G
7.2
6.4
5.6
4.8
4.0
3.2
2.4
1.6
0.8
GATA4 ChIP
6F
6F-Z
+1kb
0
-1kb
9
8
7
6
5
4
3
2
1
B
55kb
Tnni1
Lad1
Tnnt2
[0-30]
ZNF281 ChIP
6F
6F-G
GATA4 ChIP
6F
6F-Z
Cluster 1
Cluster 3
Cluster 2
C
Gene Ontology Analysis
-Log10 (p value)
Cluster 1
Cell-substrate adhesion
Cell-matrix adhesion
Substrate adhesion-dependent cell spreading
Heart growth
Pericardium development
Trabecula morphogenesis
Cardiac muscle tissue growth
Cardiac muscle cell proliferation
Cluster 2
Negative regulation of transferase activity
Negative regulation of kinase activity
Negative regulation of protein kinase activity
Regulation of muscle system process
Regulation of muscle contraction
Regulation of striated muscle contraction
Regulation of cardiac muscle contraction
Cell-substrate adhesion
Cluster 3
Response to unfolded protein
Extrinsic apoptotic signaling pathway
T cell homeostasis
PDGF receptor signaling pathway
Organelle transport along microtubule
Cell-substrate junction assembly
Actin filament bundle assembly
Apoptotic cell clearance
D
Pathway Analysis
-Log10 (p value)
TGF-beta receptor signaling
Alpha4 beta1 integrin signaling events
Stabilization and expansion of the E-cadherin adherens junction
Genes involved in CRMPs in Sema3A signaling
Genes involved in Smooth Muscle Contraction
Beta5 beta6 beta7 and beta8 integrin cell surface interactions
Wnt signaling network
Alpha9 beta1 integrin signaling events
Genes involved in Integrin cell surface interactions
ECM-receptor interaction
Beta1 integrin cell surface interactions
TGF-beta receptor signaling
Osteopontin-mediated events
Genes involved in NRAGE signals death through JNK
Genes involved in Branched-chain amino acid catabolism
Genes involved in Interleukin-6 signaling
Genes involved in Signaling by PDGF
IFN-gamma pathway
Class I PI3K signaling events
IL12-mediated signaling events
Noncanonical Wnt signaling pathway
Genes involved in GAB1 signalosome
Genes involved in Smooth Muscle Contraction
p38 MAPK signaling pathway

Figure 3-6 GATA4 recruits ZNF281 to cardiac enhancers.

(A) Heat map for ZNF281 or GATA4 at ±1 kb around the peak center in each indicating occupancy cluster. ChIP-seq experiments were performed using 2 days reprogrammed TTFs infected with 6F, 6F-G(Gata4) or 6F-Z(ZNF281). (B) IGV browser tracks at chr1:137,694,960-137,749,970 (mm9) show example of peaks that belong to each indicated clusters. (B and C) Gene ontologies (B) and pathways(C) enriched in genes that associate with each indicated clusters identified by gene ontology enrichment analysis and pathway analysis.

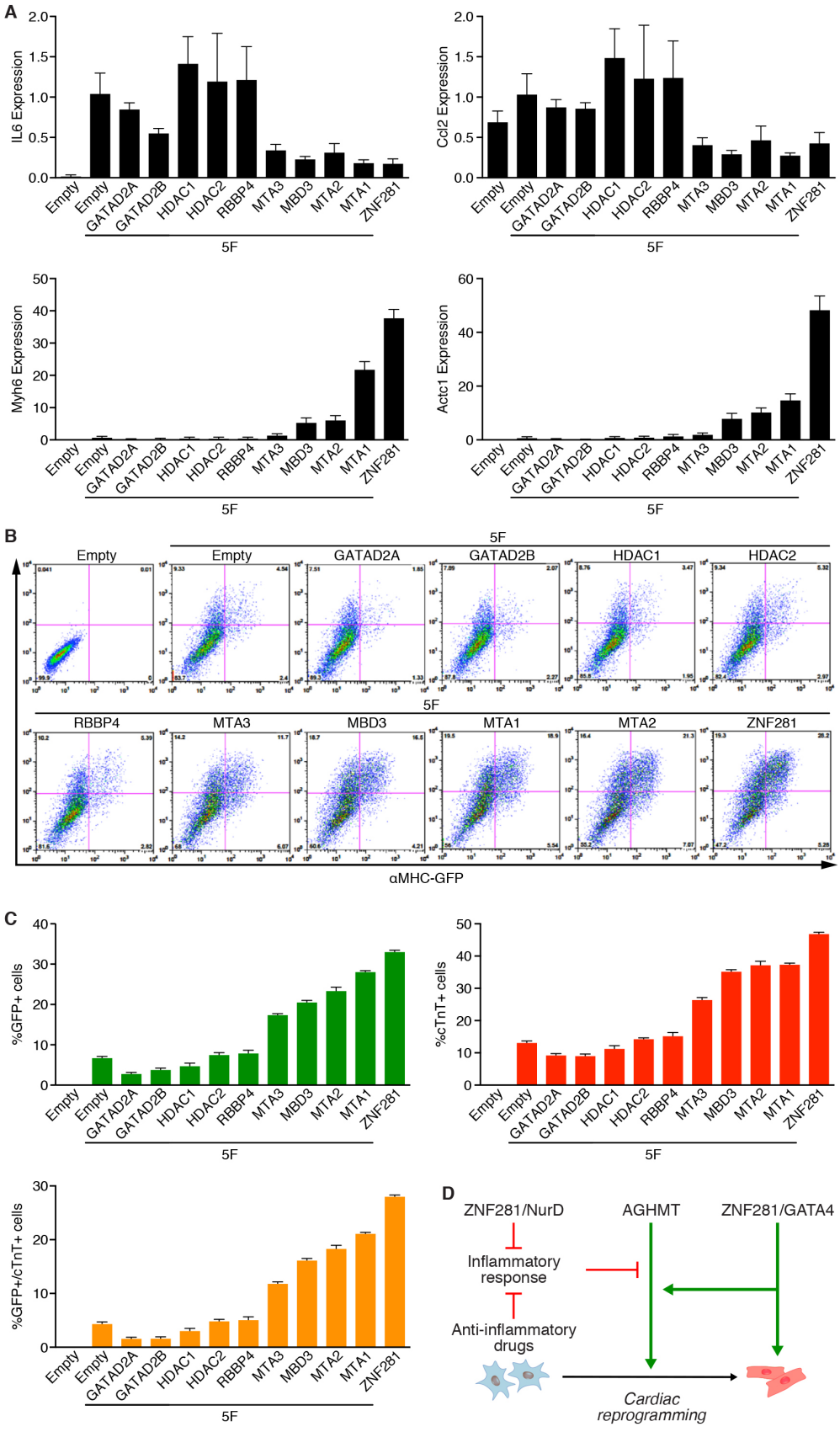
A
IL6 Expression
Ccl2 Expression
Myh6 Expression
Actc1 Expression
Empty
Empty
GATAD2A
GATAD2B
HDAC1
HDAC2
RBBP4
MTA3
MBD3
MTA2
MTA1
ZNF281
5F
B
5F
αMHC-GFP
C
%GFP+ cells
%cTnT+ cells
%GFP+/cTnT+ cells
D
ZNF281/NurD
AGHMT
ZNF281/GATA4
Inflammatory response
Anti-inflammatory drugs
Cardiac reprogramming

Figure 3-7 ZNF281 represses inflammatory response through NurD complex.

(A) TTFs were infected with Empty, 5F plus Empty, ZNF281 or each individual NurD complex subunit retroviruses for 7 days. Transcript levels of inflammatory marker genes (Il6, Ccl2) or cardiac marker genes (Myh6 and Actc1) were determined by q-PCR. (B and C) Representative flow cytometry plot (B) and analyses (C) of αMHC-GFP+ and cTnT+ cells in TTFs after 7days infection with Empty, 5F plus Empty, ZNF281 or each individual NurD complex subunit retroviruses, showing overexpressing NurD complex subunits MTA1, MTA2, MTA3 and MBD3 increase the percentage of reprogrammed cells on top of 5F. *$P<0.05$ (D) Model of ZNF281 enhances AGHMT-mediated direct cardiac reprogramming. ZNF281 is a cardiac transcription coactivator, recruited by GATA4 to cardiac enhancers to activate cardiac gene expression; ZNF281 also direct represses inflammatory response that is a barrier pathway for cardiac reprogramming

3.2 REFERENCES

1. Jessup, M., and Brozena, S. 2003. Heart failure. N Engl J Med 348:2007-2018.

2. Xin, M., Olson, E.N., and Bassel-Duby, R. 2013. Mending broken hearts: cardiac development as a basis for adult heart regeneration and repair. Nat Rev Mol Cell Biol 14:529-541.

3. Tallquist, M.D., and Molkentin, J.D. 2017. Redefining the identity of cardiac fibroblasts. Nat Rev Cardiol.

4. Fu, J.D., Stone, N.R., Liu, L., Spencer, C.I., Qian, L., Hayashi, Y., Delgado-Olguin, P., Ding, S., Bruneau, B.G., and Srivastava, D. 2013. Direct reprogramming of human fibroblasts toward a cardiomyocyte-like state. Stem Cell Reports 1:235-247.

5. Ieda, M., Fu, J.D., Delgado-Olguin, P., Vedantham, V., Hayashi, Y., Bruneau, B.G., and Srivastava, D. 2010. Direct reprogramming of fibroblasts into functional cardiomyocytes by defined factors. Cell 142:375-386.

6. Nam, Y.J., Song, K., Luo, X., Daniel, E., Lambeth, K., West, K., Hill, J.A., DiMaio, J.M., Baker, L.A., Bassel-Duby, R., et al. 2013. Reprogramming of human fibroblasts toward a cardiac fate. Proc Natl Acad Sci U S A 110:5588-5593.

7. Qian, L., Huang, Y., Spencer, C.I., Foley, A., Vedantham, V., Liu, L., Conway, S.J., Fu, J.D., and Srivastava, D. 2012. In vivo reprogramming of murine cardiac fibroblasts into induced cardiomyocytes. Nature 485:593-598.

8. Song, K., Nam, Y.J., Luo, X., Qi, X., Tan, W., Huang, G.N., Acharya, A., Smith, C.L., Tallquist, M.D., Neilson, E.G., et al. 2012. Heart repair by reprogramming non-myocytes with cardiac transcription factors. Nature 485:599-604.

9. Kojima, H., and Ieda, M. 2017. Discovery and progress of direct cardiac reprogramming. Cell Mol Life Sci 74:2203-2215.

10. Srivastava, D., and DeWitt, N. 2016. In Vivo Cellular Reprogramming: The Next Generation. Cell 166:1386-1396.

11. Vaseghi, H., Liu, J., and Qian, L. 2017. Molecular barriers to direct cardiac reprogramming. Protein Cell.

12. Zhou, H., Dickson, M.E., Kim, M.S., Bassel-Duby, R., and Olson, E.N. 2015. Akt1/protein kinase B enhances transcriptional reprogramming of fibroblasts to functional cardiomyocytes. Proc Natl Acad Sci U S A 112:11864-11869.

13. Zhou, Y., Wang, L., Vaseghi, H.R., Liu, Z., Lu, R., Alimohamadi, S., Yin, C., Fu, J.D., Wang, G.G., Liu, J., et al. 2016. Bmi1 Is a Key Epigenetic Barrier to Direct Cardiac Reprogramming. Cell Stem Cell 18:382-395.

14. Mohamed, T.M., Stone, N.R., Berry, E.C., Radzinsky, E., Huang, Y., Pratt, K., Ang, Y.S., Yu, P., Wang, H., Tang, S., et al. 2017. Chemical Enhancement of In Vitro and In Vivo Direct Cardiac Reprogramming. Circulation 135:978-995.

15. Yamakawa, H., Muraoka, N., Miyamoto, K., Sadahiro, T., Isomi, M., Haginiwa, S., Kojima, H., Umei, T., Akiyama, M., Kuishi, Y., et al. 2015. Fibroblast Growth Factors

and Vascular Endothelial Growth Factor Promote Cardiac Reprogramming under Defined Conditions. Stem Cell Reports 5:1128-1142.

16. Zhao, Y., Londono, P., Cao, Y., Sharpe, E.J., Proenza, C., O'Rourke, R., Jones, K.L., Jeong, M.Y., Walker, L.A., Buttrick, P.M., et al. 2015. High-efficiency reprogramming of fibroblasts into cardiomyocytes requires suppression of pro-fibrotic signalling. Nat Commun 6:8243.

17. Ifkovits, J.L., Addis, R.C., Epstein, J.A., and Gearhart, J.D. 2014. Inhibition of TGFbeta signaling increases direct conversion of fibroblasts to induced cardiomyocytes. PLoS One 9:e89678.

18. Muraoka, N., Yamakawa, H., Miyamoto, K., Sadahiro, T., Umei, T., Isomi, M., Nakashima, H., Akiyama, M., Wada, R., Inagawa, K., et al. 2014. MiR-133 promotes cardiac reprogramming by directly repressing Snai1 and silencing fibroblast signatures. EMBO J 33:1565-1581.

19. Abad, M., Hashimoto, H., Zhou, H., Morales, M.G., Chen, B., Bassel-Duby, R., and Olson, E.N. 2017. Notch Inhibition Enhances Cardiac Reprogramming by Increasing MEF2C Transcriptional Activity. Stem Cell Reports 8:548-560.

20. Wang, L., Liu, Z., Yin, C., Asfour, H., Chen, O., Li, Y., Bursac, N., Liu, J., and Qian, L. 2015. Stoichiometry of Gata4, Mef2c, and Tbx5 influences the efficiency and quality of induced cardiac myocyte reprogramming. Circ Res 116:237-244.

21. Yang, S.Y., Baxter, E.M., and Van Doren, M. 2012. Phf7 controls male sex determination in the Drosophila germline. Dev Cell 22:1041-1051.

22. McLean, C.Y., Bristor, D., Hiller, M., Clarke, S.L., Schaar, B.T., Lowe, C.B., Wenger, A.M., and Bejerano, G. 2010. GREAT improves functional interpretation of cis-regulatory regions. Nat Biotechnol 28:495-501.

23. Kang, C., Xu, Q., Martin, T.D., Li, M.Z., Demaria, M., Aron, L., Lu, T., Yankner, B.A., Campisi, J., and Elledge, S.J. 2015. The DNA damage response induces inflammation and senescence by inhibiting autophagy of GATA4. Science 349:aaa5612.

24. Aurora, A.B., and Olson, E.N. 2014. Immune modulation of stem cells and regeneration. Cell Stem Cell 15:14-25.

25. Lee, J., Sayed, N., Hunter, A., Au, K.F., Wong, W.H., Mocarski, E.S., Pera, R.R., Yakubov, E., and Cooke, J.P. 2012. Activation of innate immunity is required for efficient nuclear reprogramming. Cell 151:547-558.

26. Fidalgo, M., Huang, X., Guallar, D., Sanchez-Priego, C., Valdes, V.J., Saunders, A., Ding, J., Wu, W.S., Clavel, C., and Wang, J. 2016. Zfp281 Coordinates Opposing Functions of Tet1 and Tet2 in Pluripotent States. Cell Stem Cell 19:355-369.

27. Fidalgo, M., Faiola, F., Pereira, C.F., Ding, J., Saunders, A., Gingold, J., Schaniel, C., Lemischka, I.R., Silva, J.C., and Wang, J. 2012. Zfp281 mediates Nanog autorepression through recruitment of the NuRD complex and inhibits somatic cell reprogramming. Proc Natl Acad Sci U S A 109:16202-16207.

28. Perissi, V., Jepsen, K., Glass, C.K., and Rosenfeld, M.G. 2010. Deconstructing repression: evolving models of co-repressor action. Nat Rev Genet 11:109-1

CHAPTER 4. CONCLUSIONS AND FUTURE REMARKS

4.1 OPTIMIZATION OF DIRECT CARDIAC REPROGRAMMING COCKTAIL

Heart disease is the leading cause of death in the world. Direct reprogramming of fibroblasts to functional cardiomyocytes represents a potential approach for restoring cardiac function following myocardial injury. However, this reprogramming technique thus far has been relative slow and inefficient. Our initial reprogramming cocktail that consists of four cardiogenic transcription factors (GHMT) induced only ~0.02% adult TTFs to a contractile cardiomyocyte phenotype. The first aim of my PhD thesis was to improve reprogramming efficiency. We first performed a screen of 192 protein kinases and discovered that Akt dramatically enhanced and accelerated the reprogramming process in different types of fibroblasts including MEFs, CFs and TTFs. We showed that addition of Akt in the presence of GHMT (AGHMT), efficiently activates the cardiac gene program in ~50% of MEFs within three weeks. However, only ~1% of adult TTFs acquire a contractile phenotype under these conditions, suggesting the existence of barriers in adult fibroblast to the reprogramming process. Given that the major beneficiary population of this technique would be adult humans, inefficient reprogramming of adult fibroblasts to iCMs diminishes the clinical translatability of this technique.

To identify additional regulators of adult cardiac reprogramming, we carried out an unbiased screen using 1,126 open reading frame cDNAs (ORFs) encoding 700 transcription factors, 280 cytokines, 85 epigenetic regulators and 61 nuclear receptors to augment AGHMT cardiac reprogramming of ATTFs. This screen led to the discovery of 50 inducers and 133 repressors of adult cardiac reprogramming. Among the 50 identified inducers, the strongest activator of cardiac reprogramming was ZNF281, a heart enriched transcription factor. Addition

of ZNF281 to the AGHMT cocktail (AGHMTZ) converted ~30% of ATTFs to iCMs. Thus, we successfully optimized the reprogramming cocktail by adding a protein kinase AKT1 and a transcription factor, ZNF281, to the original GHMT cocktail to efficiently reprogram adult fibroblasts to cardiomyocytes.

4.2 MOLECULAR MECHANISMS OF DIRECT CARDIAC REPROGRAMMING

The second aim of my PhD thesis was to decipher the molecular mechanisms underlying direct cardiac reprogramming, especially by identifying which signaling pathways regulate this process. Understanding the molecular mechanisms of cardiac reprogramming is crucial for generating high quality iCMs and useful for therapeutic application. AKT1 is a well-studied protein kinase that is involved in various signaling pathway. We showed that Akt1 activated a pathway involving IGF1, PI3K, mTORC1 and FoxO to enhance reprogramming. The mechanism activated by AKT1 that involves mTOR and FoxO is intriguing given their roles in regulating mitochondrial metabolism, muscle development, and gene expression. The realization that Akt signaling enhances the reprogramming process raises the possibility of further augmenting this process through pharmacologic manipulation of aspects of this pathway. AGHMT-treated cells displayed changes in metabolism, mitochondria, morphology, multi/binucleation, and gene expression, corresponding to a more mature cardiomyocyte phenotype than observed in GHMT-treated cells. Cardiomyocyte multi/binucleation, as observed in response to reprogramming with AGHMT, results from progression through S-phase of the cell cycle without subsequent cytokinesis. It is interesting that Akt has been implicated in both cardiac hyperplasia and hypertrophy, depending on the specific context. It is conceivable that Akt simultaneously

stimulates hypertrophy, DNA replication, and cellular senescence similarly to development of mature/polynucleate mammalian cardiomyocytes.

Our human ORF screen led to the discovery of a total of 183 new inducers or repressors that participate in various biological pathways and processes, including transcription initiation, cell cycle regulation, chromatin modification, stress response and the inflammatory response. Interestingly, we found that anti- and pro-inflammatory factors evoke opposing effects on cardiac reprogramming. Whereas pro-inflammatory molecules prevent reprogramming, anti-inflammatory molecules profoundly enhance cardiac reprogramming. Multiple stimuli such as viral infection or expression of the pro-inflammatory gene *Gata4* can trigger the inflammatory response in cardiac reprogramming. In the clinical setting, inflammation and inflammatory cell filtration are hallmarks of MI and reperfusion injury. Ischemic cardiac injury triggers inflammatory reactions accompanied by cytokine release and inflammatory cell filtration into the infarct region. We showed that pharmacologic inhibition of the inflammatory response by anti-inflammatory drugs, dexamethasone and nabumetone, profoundly enhances cardiac reprogramming *in vitro*. Dexamethasone and nabumetone are two common anti-inflammatory drugs that have been used clinically for decades. Our findings highlight the potential clinical application of these two drugs in cardiac reprogramming.

Among the identified inducers, the zinc finger transcription factor ZNF281 showed the most potent reprogramming activity. Little is known about the functions of ZNF281. We demonstrated that the effect of ZNF281 on cardiac reprogramming was likely mediated by association with Gata4 on cardiac enhancers and by inhibition of inflammatory signaling, which antagonizes cardiac reprogramming, through the NurD complex. These findings highlight the

important roles of direct cardiac gene activation as well as the NurD complex-mediated inflammatory gene repression in the cardiac reprogramming process.

Direct reprogramming of fibroblasts to cardiomyocytes represents a distinct path to achieve the cardiac phenotype compared to embryonic stem cells or induced pluripotent stem cell derived cardiomyocytes. We showed that ZNF281 interacts with the cardiac transcription factor GATA4 to synergistically activate cardiac genes in the cardiac reprogramming process. We speculate that ZNF281 may also have important functions in the heart. The discovery of the cardiogenic function of ZNF281 in reprogramming suggests that in addition to its clinical benefit, cardiac

Our human ORF screen identified many more repressors than inducers, suggesting that fibroblasts need to overcome multiple barriers to successfully convert to iCMs. The dual role of ZNF281 in inducing cardiac reprogramming suggested that one inducer might be able to overcome multiple barriers at the same time. Many of these identified factors would not have been anticipated to impinge on the mechanisms of fibroblast-to-cardiomyocyte reprogramming. Even though my PhD thesis focused on determining the molecular mechanism of ZNF281, it will be interesting to continue to investigate how the other identified factors regulate cardiac reprogramming and the cardiac phenotype.

4.3 FUTURE DIRECTIONS OF DIRECT CARDIAC REPROGRAMMING

Considerable effort has been directed toward optimization of cardiac reprogramming cocktails and understanding the mechanism of the reprogramming process. Additional investigations are needed to translate this promising approach into clinical application.

Even though we and others have identified multiple signaling pathways as well as several biological processes that are crucial for cardiac reprogramming, the comprehensive molecular mechanism of cardiac reprogramming is still not clear. For example, little is known about how ectopic expression of GHMT drives the conversion of fibroblasts to cardiac cell types. We do know that the cardiac enhancers crucial for maintaining cardiomyocytes phenotype are closed in fibroblasts. However, it still remains to be determined which factor(s) in the reprogramming cocktail serve as pioneer factor(s) to remodel the epigenome of fibroblasts. We found ZNF281 could not bind to cardiac enhancers without GATA4, suggesting that GATA4 might the pioneer factor.

It takes weeks for fibroblasts to acquire the cardiac phenotype, even under the most optimized conditions, indicating that cardiac reprogramming is a slow process. It still needs to be determined if cardiac reprogramming is a continuous process without an intermediate state, or if there are several reprogramming phases during the reprogramming process, whereby each phase is characterized by a specific intermediate state that expresses hallmark genes. The most straightforward way to determine the phases of reprogramming would be to analyze transcriptional and epigenetic changes at different time points after AGHMTZ induction. Most recent studies have been done using a population of various fibroblasts to study the very early stage of cardiac reprogramming in which cells are relatively synchronous and homogeneous. However, it becomes challenging to gain mechanistic insight at later time points in which the cell population is asynchronous and heterogeneous. One way to overcome this problem is to use single cell sequencing techniques, such as Drop-seq or 10X genomic single cell RNA-seq, to trace the transcriptional changes over time.

Most of the recent optimization work was done using mouse fibroblasts. Reprogramming human fibroblasts requires additional factors but yields lower efficiency. The knowledge gained from mouse studies certainly will shed light on human reprogramming, however, it will be necessary to focus on human cardiac reprogramming in greater detail in the future studies, considering cardiac reprogramming as a technique to repair the human heart. Given that our ORF library consists of all human genes and our screening platform is easy to adapt to human fibroblasts. it will be of great interest to perform a human reprogramming screen using our screening platform and ORF library. Besides the reprogramming cocktail difference, the anatomy, physiology and mechanical properties between the human and mouse heart are also significantly different. In vivo reprogramming has been performed successfully using a MI-mouse model with GHMT. However, it remains to be evaluated with AGHMTZ factors. Additionally, research in a large animal model, such as pig or dog, is required to translate cardiac reprogramming into a clinical application.

A safe and efficient delivery method is a major challenge for moving cardiac reprogramming to clinical use. Proof-of-concept in vivo studies used retroviruses to deliver reprogramming factors. However, retroviruses can integrate into the genome and lead to mutagenesis and potentially, tumor formation. The ideal delivery vector should be a non-integrated vector with high packaging capacity to accommodate all the reprogramming factors. Additionally, the ideal delivery system should have high efficiency and specificity for cardiac fibroblasts but not cardiomyocytes or any other cell type. Furthermore, the ideal delivery system should be safe for human clinical trials. Unfortunately, no current gene therapeutic delivery method fulfills all listed requirements. Adeno-associated virus (AAV) is a non-integrated virus

and has been tested extensively in human clinical trials and showed safety and efficacy. However, the packaging capacity of AAV is limited to 4.7kb, which is not sufficient to accommodate all the human reprogramming factors. Moreover, no serotype of AAV that shows high specificity for cardiac fibroblasts has been identified. In fact, the most commonly used AAV serotype, AAV9, has preference for infecting cardiomyocytes over cardiac fibroblasts. Modified mRNA (modRNA) is another promising delivery method for reprogramming factors. ModRNA is currently being tested in several human clinical trials, and has no limitation for packaging capacity. However, it has low delivery efficiency and no specificity for cardiac fibroblasts. An optimized, safe and efficient delivery method for cardiac reprogramming factors needs to be developed in the future to move cardiac reprogramming into a clinical setting.

Fortunately, the in vivo reprogramming studies showed that only a small fraction of fibroblasts converted to iCMs is sufficient to partially restore cardiac function in a MI-mouse model. However, it's not clear how the efficiency of reprogramming is correlated with restoring heart function. Considering the fact that fibroblasts play an important role in both healthy and injured heart, a very efficient reprogramming might deplete endogenous cardiac fibroblasts and cause problems for heart function. An optimal efficiency of cardiac reprogramming might need to be determined in the future.